

The holographic $T\bar{T}$ deformation of the entanglement entropy in (A)dS₃/CFT₂

Jing-Cheng Chang^{a,b,c}, Song He^{d,e,f,g}, Yu-Xiao Liu^{a,b,c} and Long Zhao^f

^aKey Laboratory for Quantum Theory and Applications of MoE, Institute of Theoretical Physics and Research Center of Gravitation, Lanzhou University, Lanzhou 730000, China

^bKey Laboratory of Theoretical Physics of Gansu Province, Lanzhou Center for Theoretical Physics, Lanzhou University, Lanzhou 730000, China

^cSchool of Physical Science and Technology, Lanzhou University, Lanzhou 730000, China

^dInstitute of Fundamental Physics and Quantum Technology, Ningbo University, Ningbo, Zhejiang 315211, China

^eSchool of Physical Science and Technology, Ningbo University, Ningbo, 315211, China

^fCenter for Theoretical Physics and College of Physics, Jilin University, Changchun 130012, People's Republic of China

^gMax Planck Institute for Gravitational Physics (Albert Einstein Institute), Am Mühlenberg 1, 14476 Golm, Germany

E-mail: 120220908561@lzu.edu.cn, hesong@jlu.edu.cn, liuyx@lzu.edu.cn, zhaolong@jlu.edu.cn

ABSTRACT: In recent years, the holographic duality between $T\bar{T}$ -deformed conformal field theory (CFT) and Anti-de Sitter (AdS) space with finite radial truncation has received significant attention. The study of $T\bar{T}$ deformation within the framework of de Sitter (dS)/CFT duality has also progressed. This paper shows that the trace flow equation in dS spacetime can be analytically extended from its AdS counterpart through double Wick rotations. Additionally, we generalize the replica sphere method in both AdS and dS holography to derive a general expression for the entanglement entropy of arbitrary single spatial intervals. For both finite size and finite temperature systems, we obtain the entanglement entropy corrections due to $T\bar{T}$ deformation. Finally, using strong subadditivity and boosted strong subadditivity, we show that the dual field theory on the timelike boundary is non-local in dS holography.

KEYWORDS: Entanglement entropy, $T\bar{T}$ deformation, AdS holography, dS holography.

Contents

1	Introduction	1
2	Holographic $T\bar{T}$ Flow	4
2.1	$T\bar{T}$ Flow in AdS/CFT	4
2.2	$T\bar{T}$ Flow in dS/CFT	6
2.3	Double Wick Rotation to dS/CFT	7
3	The Replica Method for the $T\bar{T}$-Deformed Field Theory	8
3.1	AdS case	9
3.2	dS case	11
4	Entanglement entropy for arbitrary single spatial intervals	14
4.1	The generalization of the replica method	14
4.2	System with finite size	19
4.3	System with finite temperature	22
5	(A)dS/dS case and non-locality	25
5.1	AdS/dS	25
5.2	dS/dS	26
5.3	The half-dS holography	29
6	Conclusion and Discussion	32
A	The gravity calculation	33
A.1	The dS/Poincaré case	33
A.2	The global dS case	34

1 Introduction

The $T\bar{T}$ deformation [1, 2] of conformal field theory (CFT) is an irrelevant deformation that exhibits factorization properties in the large central charge limit [3, 4]. For a two-dimensional CFT, the $T\bar{T}$ deformation is defined by the double trace operator

$$\frac{dS}{d\lambda} = 2\pi \int d^2x \sqrt{g} T\bar{T}, \quad T\bar{T} \equiv \frac{1}{8}(T^{ij}T_{ij} - (T_i^i)^2). \quad (1.1)$$

The strength of this deformation is controlled by the deformation parameter λ . If we treat the deformation as a perturbation and expand the deformed theory to first-order in the deformation parameter λ , we obtain

$$S_{\text{QFT}} \simeq S_{\text{CFT}} + 2\pi\lambda \int d^2x \sqrt{g} T\bar{T}. \quad (1.2)$$

From the perspective of the AdS/CFT duality [5–7], the $T\bar{T}$ -deformed CFT corresponds to the semi-classical gravity theory living in an AdS spacetime with finite cutoff [8, 9], as shown in figure 1.

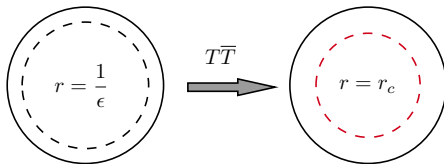


Figure 1. The holography $T\bar{T}$ deformation. The black solid circle represents the AdS boundary, the black dashed circle represents the cutoff at the asymptotic boundary $r = \frac{1}{\epsilon}$, and the red dashed circle represents the finite cutoff $r = r_c$.

In refs. [8, 9], the authors calculated the propagation speed of the massless modes, energy spectrum, and partition functions in both the contexts of the $T\bar{T}$ -deformed quantum field theory and AdS gravity with a finite cutoff. The generic holographic correlation functions have been established in the refs. [10–13]. These results support the duality depicted in figure 1. In addition to the aforementioned correspondences, another significant result of holographic principles is that the entanglement entropy of the boundary field theory equals the area of the minimal surface, also known as the Ryu-Takayanagi (RT) surface, inside the AdS spacetime [14, 15]. The RT formula for holographic entanglement entropy serves as a criterion for validating the holographic principle, with $T\bar{T}$ -deformed theories offering an additional test. For the holographic duality with $T\bar{T}$ deformation, this duality has been discussed in refs. [16–22]. In ref. [16], the authors investigated the entanglement entropy of the $T\bar{T}$ -deformed field theory at the level of perturbation (1.2). They found that for the system at finite temperature, the entanglement entropy receives a first-order λ correction from the $T\bar{T}$ deformation, but for a system of finite size, this first-order correction disappears. To explore the impact of $T\bar{T}$ deformation on the entanglement entropy in finite-size systems, ref. [23] examined the timelike entanglement entropy, drawing similar conclusions to previous studies [24, 25]. They found that the timelike entanglement entropy receives no first-order correction at finite temperature, but there is a first-order correction in the finite size case. Additionally, the reflected entropy [26] and pseudo entropy [27] of the $T\bar{T}$ deformed field theory have been studied in refs. [28, 29]. For more interesting work on $T\bar{T}$ deformation, please refer to refs. [30–42].

The holographic principle has been well established in the AdS spacetime with finite cutoff $r = r_c$. However, given that our real universe is more accurately described by a dS metric,

it is crucial to explore whether the holographic principle extends to the dS spacetime [43–49]. In the usual dS/CFT duality [50, 51], the CFT resides on a future spacelike boundary, which renders the dual field theory non-unitary [44, 52]. Due to the challenges of the dS/CFT duality [53, 54], there are only a few clearly established examples [55–57]. In recent years, other holographic duality models in the dS spacetime, such as the dS/dS correspondence [58–64] and half-dS holography [65], have gained attention and been studied. In these two models, the holographic boundary is a timelike boundary of the dS spacetime, so the dual field theory is expected to be unitary. In the dS/dS correspondence, the cosmological constant term also appears in the trace flow equation of the $T\bar{T}$ deformation, thus the $T\bar{T}$ deformation of this model is referred to as $T\bar{T} + \Lambda_2$ deformation [66–70].

We aim to study the impact of $T\bar{T}$ deformation on the entanglement entropy in the dS/CFT duality. However, the deformed field theory no longer retains conformal symmetry, rendering the original method for calculating the entanglement entropy inapplicable. Fortunately, when the deformed CFT is situated on a two-dimensional sphere, the entanglement entropy of a subregion with endpoints at antipodal points can be calculated via the replica method [71–74]. In this context, by adjusting the spherical radius r , we can study the renormalization group flow [75, 76] of the dual field theory under $T\bar{T}$ deformation, with r functioning as the radial coordinate in the bulk spacetime. This method is an extension of the approach proposed in ref. [77] and was further generalized in ref. [78] to compute the entanglement entropy of arbitrary spatial intervals on a two-dimensional plane. In ref. [79], the replica method was employed within the $T\bar{T}$ -deformed dS/CFT duality to calculate the entanglement entropy for the subregion between two antipodal points on the sphere.

In this paper, we present a general expression for the entanglement entropy of arbitrary spatial intervals in both AdS and dS holography by combining the Casini-Huerta-Myers (CHM) map [80] with the replica method on a sphere. The results are

- AdS($0 < r_{\text{eff}} < \infty$): $S = \frac{c_{\text{AdS}}}{3} \operatorname{arctanh} \left(\frac{1}{\sqrt{1 + \frac{c_{\text{AdS}} \lambda_{\text{AdS}}}{12r_{\text{eff}}^2}}} \right),$
- dS($\ell_{\text{dS}} < r_{\text{eff}} < \infty$): $S = -\frac{ic_{\text{dS}}}{3} \operatorname{arccoth} \left(\frac{1}{\sqrt{1 - \frac{c_{\text{dS}} \lambda_{\text{dS}}}{12r_{\text{eff}}^2}}} \right) + \frac{\pi c_{\text{dS}}}{6},$
- dS($0 < r_{\text{eff}} < \ell_{\text{dS}}$): $S = \frac{c_{\text{dS}}}{3} \operatorname{arctan} \left(\frac{1}{\sqrt{\frac{c_{\text{dS}} \lambda_{\text{dS}}}{12r_{\text{eff}}^2} - 1}} \right),$

where $\ell_{(\text{A})\text{dS}}$ represents the (A)dS radius, $c_{(\text{A})\text{dS}} = \frac{3\ell_{(\text{A})\text{dS}}}{2G}$ is the Brown-Henneaux central charge [81], $\lambda_{(\text{A})\text{dS}} = 8G\ell_{(\text{A})\text{dS}}$ is the $T\bar{T}$ deformation parameter¹ and r_{eff} denotes the effective radius of the sphere, which is related to the size of the subsystem. In the case of dS holography,

¹As mentioned in ref. [72], we adopt the same unit system. The factor r_c , which distinguishes the CFT metric from the induced bulk metric, is absorbed into the effective radius r_{eff} of the sphere.

we find that the results for the holographic entanglement entropy can be summarized in a single formula:

$$S = -\frac{ic_{\text{dS}}}{3} \operatorname{arctanh} \left(\frac{1}{\sqrt{1 - \frac{c_{\text{dS}} \lambda_{\text{dS}}}{12r_{\text{eff}}^2}}} \right). \quad (1.3)$$

When the effective radius of the sphere is greater than the cosmological horizon radius ($\ell_{\text{dS}} < r_{\text{eff}} < \infty$), this formula corresponds to the result of the $T\bar{T}$ -deformed dS/CFT duality, where the dual field theory is non-unitary. When the effective radius of the sphere is less than the cosmological horizon radius ($0 < r_{\text{eff}} < \ell_{\text{dS}}$), this formula agrees with the results of dS/dS correspondence and half-dS holography, where the dual field theory is non-local [62, 63, 65].

This paper is organized as follows: In Section 2, we review the results from ref. [9] to derive the trace flow equations in AdS/CFT with Euclidean signature and in dS/CFT with Lorentzian signature. We then demonstrate the extension from one result to the other via a double Wick rotation. In Section 3, we review the calculation of the entanglement entropy of the $T\bar{T}$ -deformed CFT, providing general expressions for both AdS and dS holographies. Based on these findings, we calculate the C -function and discuss the non-unitarity and non-locality of the dual field theory. In Section 4, we review and generalize the CHM method for calculating the entanglement entropy of arbitrary spatial intervals in the $T\bar{T}$ -deformed theory. We explore the effects of the $T\bar{T}$ deformation in finite temperature and finite size systems. In Section 5, we first verify the calculation of the entanglement entropy in the AdS/dS correspondence. We then examine the non-locality of the dual field theory in dS/dS correspondence and half-dS holography by analyzing the strong subadditivity and the boosted strong subadditivity. Finally, we summarize our results and present a discussion in Section 6.

2 Holographic $T\bar{T}$ Flow

In this section, we review the holographic derivation of the trace flow equation for the $T\bar{T}$ deformation [82, 83]. We then show that the trace flow equation in the dS/CFT duality can be obtained from its AdS counterpart via a double Wick rotation.

2.1 $T\bar{T}$ Flow in AdS/CFT

The action for Einstein gravity in Euclidean AdS₃ (EAdS₃) spacetime \mathcal{M} , with a boundary $\partial\mathcal{M}$ at a finite radial cutoff, is given by

$$S = \frac{1}{16\pi G} \int_{\mathcal{M}} d^3x \sqrt{g} \left(\mathcal{R}^{(3)} + \frac{2}{\ell_{\text{AdS}}^2} \right) + \frac{1}{8\pi G} \int_{\partial\mathcal{M}} d^2x \sqrt{\gamma} \left(K - \frac{1}{\ell_{\text{AdS}}} \right), \quad (2.1)$$

where K denotes the trace of the extrinsic curvature of the timelike boundary $\partial\mathcal{M}$. The quasi-local stress tensor [84] is defined as the variation of the on-shell action with respect to the induced boundary metric γ^{ij} ,

$$T_{ij} = \frac{2}{\sqrt{\gamma}} \frac{\delta S}{\delta \gamma^{ij}} = \frac{1}{8\pi G} \left(K_{ij} - K \gamma_{ij} + \frac{1}{\ell_{\text{AdS}}} \gamma_{ij} \right). \quad (2.2)$$

The EAdS₃ metric in Fefferman-Graham [85] coordinates is

$$ds^2 = \frac{\ell_{\text{AdS}}^2}{r^2} (dr^2 + h_{ij} dx^i dx^j), \quad \gamma_{ij} = \frac{\ell_{\text{AdS}}^2}{r_c^2} h_{ij}. \quad (2.3)$$

In these coordinates, the spacetime is foliated by hypersurfaces labeled by the radial coordinate r . The extrinsic curvature of the hypersurface Σ_{r_c} at $r = r_c$ is given by

$$K_{ij} = \frac{1}{2} n^r \partial_r \left(\frac{\ell_{\text{AdS}}^2}{r^2} h_{ij} \right) \Big|_{r=r_c} = \frac{r}{2\ell_{\text{AdS}}} \partial_r \left(\frac{\ell_{\text{AdS}}^2}{r^2} h_{ij} \right) \Big|_{r=r_c}, \quad (2.4)$$

where n^r is the outward-pointing normal vector to the hypersurface Σ_{r_c} . The (r, r) component of Einstein's equations is

$$K^2 - K_{ij} K^{ij} = \mathcal{R}^{(2)} + \frac{2}{\ell_{\text{AdS}}^2}, \quad (2.5)$$

where $\mathcal{R}^{(2)}$ is the Ricci scalar of the hypersurface Σ_{r_c} . Substituting the expression for K_{ij} from eq. (2.2) into eq. (2.5) yields the trace flow equation

$$T^i_i = -\frac{\ell_{\text{AdS}}}{16\pi G} \mathcal{R}^{(2)} - 4\pi G \ell_{\text{AdS}} [T^{ij} T_{ij} - (T^i_i)^2]. \quad (2.6)$$

Equation (2.5) is equivalent to the Hamiltonian constraint $H = 0$ in the canonical form of Einstein's gravity theory [86], with the Hamiltonian given by

$$H = \frac{16\pi G}{\sqrt{\gamma}} [\Pi^{ij} \Pi_{ij} - (\Pi^i_i)^2] + \frac{\sqrt{\gamma}}{16\pi G} \left(\mathcal{R}^{(2)} + \frac{2}{\ell_{\text{AdS}}^2} \right) = 0, \quad (2.7)$$

where Π^{ij} is the canonical momentum defined as

$$\Pi^{ij} = \frac{\sqrt{\gamma}}{16\pi G} (K \gamma^{ij} - K^{ij}). \quad (2.8)$$

In the canonical form of quantum gravity with Euclidean signature, the wavefunction of the induced metric γ_{ij} on the hypersurface Σ_{r_c} can be written as $\Psi \equiv e^{-S}$, where S is the classical action of Einstein gravity with the Gibbons-Hawking-York boundary term. After renormalization by introducing a counterterm, the wavefunction takes the form [87]

$$\Psi = \exp \left(-\frac{1}{8\pi G \ell_{\text{AdS}}} \int_{\partial\mathcal{M}} d^2x \sqrt{\gamma} \right) \hat{\Psi}. \quad (2.9)$$

This corresponds to performing a canonical transformation on the conjugate momentum

$$\Pi^{ij} \rightarrow \Pi^{ij} + \frac{\sqrt{\gamma}}{16\pi G \ell_{\text{AdS}}} \gamma^{ij}. \quad (2.10)$$

The Wheeler-DeWitt equation $H \hat{\Psi} = 0$ [88] in terms of the original conjugate momentum becomes

$$\begin{aligned} H \hat{\Psi} &= \left(\frac{16\pi G}{\sqrt{\gamma}} (\Pi^{ij} \Pi_{ij} - (\Pi^i_i)^2) - \frac{2}{\ell_{\text{AdS}}} \Pi + \frac{\sqrt{\gamma}}{16\pi G} \mathcal{R}^{(2)} \right) \hat{\Psi}, \\ &= \sqrt{\gamma} \left(4\pi G (T^{ij} T_{ij} - (T^i_i)^2) + \frac{1}{\ell_{\text{AdS}}} T^i_i + \frac{\mathcal{R}^{(2)}}{16\pi G} \right) \hat{\Psi} = 0, \end{aligned} \quad (2.11)$$

where in the second line we have used the relation $T^{ij} = -\frac{2}{\sqrt{\gamma}}\Pi^{ij}$. This aligns with the trace flow equation (2.6). To match this with the CFT trace flow equation

$$T^i_i = -\frac{c}{24\pi}\mathcal{R}^{(2)} - 4\pi\lambda T\bar{T}, \quad (2.12)$$

we require the central charge c and the deformation parameter λ to be

$$\text{AdS: } c = \frac{3\ell_{\text{AdS}}}{2G} = c_{\text{AdS}}, \quad \lambda = 8G\ell_{\text{AdS}} = \lambda_{\text{AdS}}. \quad (2.13)$$

2.2 $T\bar{T}$ Flow in dS/CFT

In the dS/CFT duality, the holographic direction corresponds to time, so the dS metric in Fefferman-Graham coordinates is given by

$$ds^2 = \frac{\ell_{\text{dS}}^2}{r^2}(-dr^2 + h_{ij}dx^i dx^j), \quad \gamma_{ij} = \frac{\ell_{\text{dS}}^2}{r_c^2}h_{ij}, \quad (2.14)$$

where r is the holographic coordinate. The holographic boundary Σ_{r_c} , determined by $r = r_c$, is spacelike. The bulk geometry has a Lorentzian signature, and its gravitational partition function is assumed to be the Bunch-Davies wavefunction [52, 55]. Thus, according to the holographic dictionary, the partition function of the CFT is

$$\Psi_{\text{dS}} = Z_{\text{QFT}} = e^{iS_{\text{dS}}}, \quad (2.15)$$

where S_{dS} is the on-shell action of Einstein gravity with the dS geometry,

$$S_{\text{dS}} = \frac{1}{16\pi G} \int_{\mathcal{M}} d^3x \sqrt{-g} \left(\mathcal{R}^{(3)} - \frac{2}{\ell_{\text{dS}}^2} \right) + \frac{1}{8\pi G} \int_{\partial\mathcal{M}} d^2x \sqrt{\gamma} \left(K - \frac{1}{\ell_{\text{dS}}} \right). \quad (2.16)$$

The trace flow equation for the dS/CFT case can be derived using a method parallel to that of the AdS/CFT case. First, we define the renormalized wavefunction by introducing boundary counterterms, corresponding to a canonical transformation on the conjugate momentum

$$\Psi_{\text{dS}} = \exp\left(\frac{i}{8\pi G\ell_{\text{dS}}} \int_{\partial\mathcal{M}} d^2x \sqrt{\gamma}\right) \hat{\Psi}_{\text{dS}}, \quad \Pi_{\text{dS}}^{ij} \rightarrow \Pi_{\text{dS}}^{ij} + \frac{\sqrt{\gamma}}{16\pi G\ell_{\text{dS}}}\gamma^{ij}. \quad (2.17)$$

The Wheeler-DeWitt equation for the renormalized wavefunction, expressed in terms of the original conjugate momentum, is

$$\begin{aligned} H\hat{\Psi}_{\text{dS}} &= \left[\frac{16\pi G}{\sqrt{\gamma}}(\Pi^{ij}\Pi_{ij} - (\Pi^i_i)^2) - \frac{2}{\ell_{\text{dS}}}\Pi - \frac{\sqrt{\gamma}}{16\pi G}\mathcal{R}^{(2)} \right] \hat{\Psi}_{\text{dS}} \\ &= \sqrt{\gamma} \left(-4\pi G(T^{ij}T_{ij} - (T^i_i)^2) - \frac{i}{\ell_{\text{dS}}}T^i_i - \frac{\mathcal{R}^{(2)}}{16\pi G} \right) \hat{\Psi}_{\text{dS}} = 0, \end{aligned} \quad (2.18)$$

where $T^{ij} = -\frac{2i}{\sqrt{\gamma}}\Pi^{ij}$. This leads to the $T\bar{T}$ trace flow equation for the dS/CFT is

$$T^i_i = \frac{i\ell_{\text{dS}}}{16\pi G}\mathcal{R}^{(2)} + i4\pi G\ell_{\text{dS}}(T^{ij}T_{ij} - (T^i_i)^2). \quad (2.19)$$

By comparing this with the field theory equation, the correspondences between the Brown-Henneaux central charge, the deformation parameter, and the gravitational quantities for the dS spacetime [79] are given by

$$c = -i \frac{3\ell_{\text{AdS}}}{2G} = -ic_{\text{dS}}, \quad \lambda = -i8G\ell_{\text{AdS}} = -i\lambda_{\text{dS}}. \quad (2.20)$$

2.3 Double Wick Rotation to dS/CFT

In this subsection, we demonstrate that the trace flow equation for the dS/CFT, given by eq. (2.19), can be derived by performing a double Wick rotation on the trace flow equation for the AdS/CFT, given by eq. (2.6). The double Wick rotation is defined by

$$\ell_{\text{AdS}} \rightarrow -i\ell_{\text{dS}}, \quad r \rightarrow -ir. \quad (2.21)$$

The transformations of various components in the partition function under the double Wick rotation are summarized in Table 1².

Table 1. Analytical continuation from EAdS to dS

EAdS	dS	Analytical Continuation
$n_a^{(\text{AdS})} = \frac{\ell_{\text{AdS}}}{r} (dr)_a$	$n_a^{(\text{dS})} = \frac{\ell_{\text{dS}}}{r} (dr)_a$	$n_a^{(\text{AdS})} \rightarrow -in_a^{(\text{dS})}$
$n_{(\text{AdS})}^a = \frac{r}{\ell_{\text{AdS}}} \left(\frac{\partial}{\partial r}\right)^a$	$n_{(\text{dS})}^a = -\frac{r}{\ell_{\text{dS}}} \left(\frac{\partial}{\partial r}\right)^a$	$n_{(\text{AdS})}^a \rightarrow -in_{(\text{dS})}^a$
$K_{ab}^{(\text{AdS})} = \frac{1}{2} n^r \partial_r g_{ab}$	$K_{ab}^{(\text{dS})} = -\frac{1}{2} n^r \partial_r g_{ab}$	$K_{ab}^{(\text{AdS})} \rightarrow iK_{ab}^{(\text{dS})}$
$\epsilon_{abc}^{(\text{AdS})} = \sqrt{g} (dr)_a \wedge (d\tau)_b \wedge (dx)_c$	$\epsilon_{abc}^{(\text{dS})} = \sqrt{-g} (dr)_a \wedge (d\tau)_b \wedge (dx)_c$	$\epsilon_{abc}^{(\text{AdS})} \rightarrow -i\epsilon_{abc}^{(\text{dS})}$
$\epsilon_{ab}^{(\text{AdS})} = n_{(\text{AdS})}^a \epsilon_{abc}^{(\text{AdS})}$	$\epsilon_{ab}^{(\text{dS})} = n_{(\text{dS})}^a \epsilon_{abc}^{(\text{dS})}$	$\epsilon_{ab}^{(\text{AdS})} \rightarrow -\epsilon_{ab}^{(\text{dS})}$
$\mathcal{R}_{(\text{AdS})}^{(3)} = -\frac{6}{\ell_{\text{AdS}}^2}$	$\mathcal{R}_{(\text{dS})}^{(3)} = \frac{6}{\ell_{\text{dS}}^2}$	$\mathcal{R}_{(\text{AdS})}^{(3)} \rightarrow \mathcal{R}_{(\text{dS})}^{(3)}$
$S_{ct}^{(\text{AdS})}$	$S_{ct}^{(\text{dS})}$	$S_{ct}^{(\text{AdS})} \rightarrow -iS_{ct}^{(\text{dS})}$

By applying the transformation rules in Table 1 to the on-shell action of AdS gravity (2.1), we obtain the on-shell action for dS gravity, multiplied by an imaginary factor i :

$$\begin{aligned} S_{\text{AdS}} &\rightarrow -\frac{i}{16\pi G} \int_{\mathcal{M}} d^3x \sqrt{-g} \left(\mathcal{R}^{(3)} - \frac{2}{\ell_{\text{dS}}^2} \right) \\ &\quad - \frac{1}{8\pi G} \int_{\partial\mathcal{M}} d^2x \sqrt{\gamma} \left(iK - \frac{i}{\ell_{\text{dS}}} \right) \\ &= -iS_{\text{dS}}. \end{aligned} \quad (2.22)$$

The double Wick rotation implies that the partition function of AdS gravity corresponds to the Bunch-Davies wavefunction of dS gravity. Additionally, all quantities in the Wheeler-DeWitt equation for the AdS spacetime are mapped to their corresponding quantities in the Wheeler-DeWitt equation for the dS spacetime. As a result, eqs. (2.9) and (2.11) correspond to eqs. (2.17) and (2.18), respectively. Therefore, the trace flow equation in the dS/CFT can be directly derived by applying this rotation to the trace flow equation in the AdS/CFT.

²Note that for the general dS/CFT, where the CFT resides on the infinite spacelike boundary, the external curvature must be defined using the inward normal vector.

3 The Replica Method for the $T\bar{T}$ -Deformed Field Theory

This section reviews the replica trick for calculating the entanglement entropy of the subregion between two antipodal points on a two-dimensional sphere [72, 79]. The sphere serves as the background manifold for the $T\bar{T}$ -deformed CFT, with its radius linked to the deformation parameter from a holographic perspective. In the dS/CFT correspondence, the CFT resides on a future spacelike boundary, which is also a two-dimensional sphere in global dS coordinates. Thus, the replica method applied in the AdS case is equally applicable in the dS case.

The metric that describes the boundary two-dimensional sphere in both AdS and dS cases is

$$ds^2 = \gamma_{ab} dx^a dx^b = r^2 (d\theta^2 + \sin^2 \theta d\phi^2), \quad (3.1)$$

where r represents the effective radius of the boundary sphere. The replica trick is used to compute the entanglement entropy of the subregion A , defined between the antipodal points $\theta = 0$ and $\theta = \pi$ at $\phi = \text{constant}$, as illustrated in figure 2.

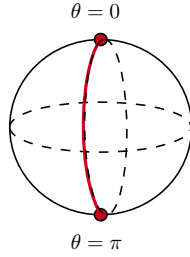


Figure 2. The meridian at $\phi = \text{constant}$ with endpoints at antipodal points defines the subregion A .

By performing n copies along the meridian at $\phi = \text{constant}$, the n -replica geometry is obtained [77, 89] by

$$ds_n^2 = r^2 (d\theta^2 + n^2 \sin^2 \theta d\phi^2). \quad (3.2)$$

The entanglement entropy of the subregion A is computed by taking the limit $n \rightarrow 1$ of the conical entropy [77, 90, 91]

$$S_A = \lim_{n \rightarrow 1} \left(1 - n \frac{\partial}{\partial n} \right) \ln Z_n, \quad (3.3)$$

where Z_n is the partition function of the field theory on the n -replica geometry. Based on the definition of the stress tensor, the following expressions hold

$$\frac{d}{dr} \ln Z_n = - \int_{\mathbb{S}_n^2} d^2x \frac{\delta \mathcal{L}}{\delta g_{ab}} \frac{dg_{ab}}{dr} = - \frac{1}{r} \int_{\mathbb{S}_n^2} d^2x \sqrt{g} T^{ab} g_{ab}, \quad (3.4)$$

and

$$\frac{\partial}{\partial n} \ln Z_n = - \int_{\mathbb{S}_n^2} d^2x \frac{\delta \mathcal{L}}{\delta g_{\phi\phi}} \frac{\partial g_{\phi\phi}}{\partial n} = - \frac{1}{n} \int_{\mathbb{S}_n^2} d^2x \sqrt{g} T^{\phi\phi} g_{\phi\phi}. \quad (3.5)$$

The trace flow equation and the conservation equation determine the stress tensor as follows:

$$\begin{cases} T^a_a = -\frac{c}{24\pi}R^{(2)} - \frac{\pi\lambda}{2} [T^{ab}T_{ab} - (T^a_a)^2], \\ \nabla_a T^a_b = 0. \end{cases} \quad (3.6)$$

Due to the maximal symmetry of the geometry, the quasi-local stress tensor is assumed to take the form

$$T_{ab} = \alpha\gamma_{ab}, \quad T^\theta_\theta = T^\phi_\phi = \frac{1}{2}\text{tr} T. \quad (3.7)$$

Under these assumptions, it follows that $\frac{d\ln Z_n}{dr}\big|_{n=1} = -8\pi r\alpha$, and the entanglement entropy of the subregion A is given by

$$S_A = \lim_{n \rightarrow 1} \left(1 - \frac{r}{2} \frac{d}{dr}\right) \ln Z_n. \quad (3.8)$$

In this case, the parameter α determines the stress tensor, which is uniquely defined by the trace flow equations. This approach is specifically designed to calculate the entanglement entropy of the subregion between two antipodal points on the sphere. Future work aims to extend this framework to explore broader implications of the holographic principle, building on the refs. [78, 92].

3.1 AdS case

By substituting the assumed form of the stress tensor $T_{ij} = \alpha\gamma_{ij}$ into eq. (2.6), the equation for α is obtained as

$$8\pi G\ell_{\text{AdS}}\alpha^2 = 2\alpha + \frac{\ell_{\text{AdS}}}{16\pi G}\mathcal{R}^{(2)}, \quad (3.9)$$

where $\mathcal{R}^{(2)} = \frac{2}{r^2}$ for the two-dimensional sphere (3.1). The solution to this equation is given by

$$\alpha = \frac{1}{\pi\lambda_{\text{AdS}}} \left(1 - \sqrt{1 + \frac{\lambda_{\text{AdS}}c_{\text{AdS}}}{12r^2}}\right). \quad (3.10)$$

Substituting this expression for α into eq. (3.4), the n -replica partition function Z_n can be computed by integrating with respect to α :

$$\ln Z_n = \frac{c_{\text{AdS}}}{3} \text{arctanh} \left(\frac{1}{\sqrt{1 + \frac{c_{\text{AdS}}\lambda_{\text{AdS}}}{12r^2}}} \right) + \frac{4r^2}{\lambda_{\text{AdS}}} \left(-1 + \sqrt{1 + \frac{c_{\text{AdS}}\lambda_{\text{AdS}}}{12r^2}} \right). \quad (3.11)$$

The entanglement entropy of the subregion A is then obtained as

$$S_A = \lim_{n \rightarrow 1} \left(1 - \frac{r}{2} \frac{d}{dr}\right) \log Z_n = \frac{c_{\text{AdS}}}{3} \text{arctanh} \left(\frac{1}{\sqrt{1 + \frac{c_{\text{AdS}}\lambda_{\text{AdS}}}{12r^2}}} \right). \quad (3.12)$$

The entanglement entropy between two antipodal points on a sphere reflects the number of degrees of freedom in the field theory defined on the sphere [93]. Casini and Huerta, using the principles of unitarity and locality in quantum field theory (QFT), demonstrated that the C -function, which measures the degrees of freedom, exhibits a monotonically decreasing behavior along the renormalization group flow for unitary and Lorentz-invariant QFTs [94–96]. This validates Zamolodchikov’s C -theorem [97]. Since the $T\bar{T}$ trace flow equation is equivalent to the holographic renormalization group flow equation, the renormalization group flow can be controlled by adjusting the radius of the sphere [98–103]. In the AdS case, the C -function is given by

$$C(r) = 3rS'_A(r) = c_{\text{AdS}} \frac{1}{\sqrt{1 + \frac{c_{\text{AdS}}\lambda_{\text{AdS}}}{12r^2}}}. \quad (3.13)$$

As illustrated in figure 3, the C -function decreases monotonically as r decreases, consistent with the number of degrees of freedom decreases along the renormalization group flow. Additionally, as r approaches infinity, the C -function converges to the central charge of the two-dimensional CFT, indicating that the renormalization group flow approaches the UV fixed point [104]. This behavior is in agreement with the C -theorem.

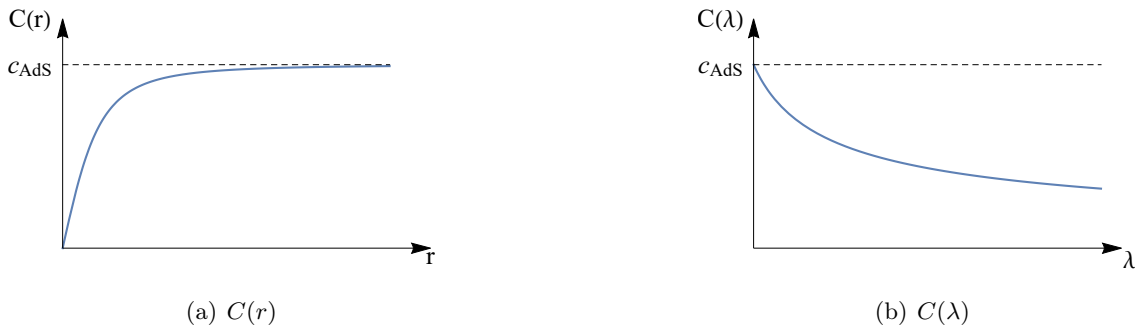


Figure 3. The C -function of the AdS spacetime. We use $\lambda = \frac{\lambda_{\text{AdS}}}{r^2}$ to represent the deformation parameter. As the boundary cutoff $r = r_c$ is pushed further into the bulk, the deformation parameter increases and the theory deviates from the CFT increasingly.

The C -theorem can be proven using locality and unitarity, but the converse is not true. Therefore, the locality of the field theory is next examined through the strong subadditivity inequality and the boosted strong subadditivity inequality. The strong subadditivity inequality is given by

$$S(A) + S(B) - S(A \cup B) - S(A \cap B) \geq 0, \quad (3.14)$$

where the subsystems A and B are shown in figure 4(a). In the limit where $A \rightarrow B$ and $|A| = |B| = L$, the strong subadditivity inequality can be expressed in its infinitesimal form as

$$L^2 S''(L) \leq 0, \quad (3.15)$$

where L represents the size of the subsystems.

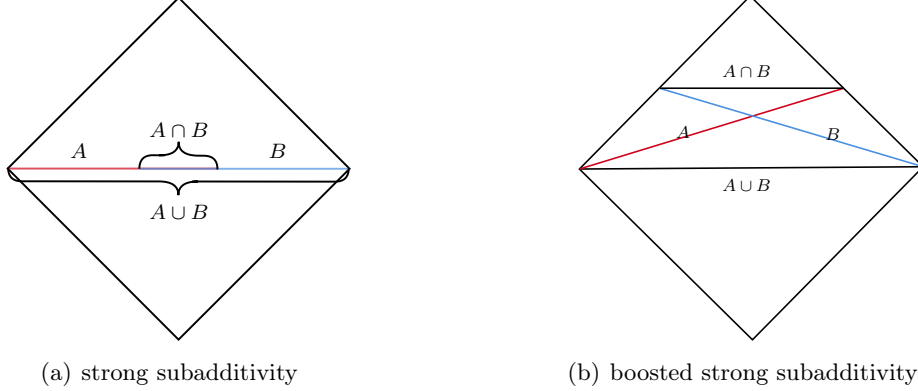


Figure 4. The left figure shows two spatial regions A and B at $t = 0$. The right figure considers the regions A and B after a boost, resulting in two spacelike regions.

A stronger criterion for proving locality, compared to the strong subadditivity, is the boosted strong subadditivity, which can be derived by applying a boost transformation to subsystems A and B , as shown in figure 4(b). The infinitesimal form of the boosted strong subadditivity inequality is expressed as

$$L^2 S''(L) + L S'(L) \leq 0. \quad (3.16)$$

Since the subsystems correspond to great arcs between antipodal points on a sphere, their size is proportional to the sphere's radius, i.e., $L = \pi r$. Consequently, the derivatives with respect to L in the strong subadditivity and the boosted strong subadditivity inequalities are equivalent to derivatives with respect to r . Taking the second derivative of eq. (3.12) with respect to r yields the strong subadditivity inequality

$$r^2 \partial_r^2 S_A(r) = - \frac{c_{\text{AdS}}}{3 \left(1 + \frac{c_{\text{AdS}} \lambda_{\text{AdS}}}{12 r^2} \right)^{\frac{3}{2}}} < 0. \quad (3.17)$$

This result shows that the strong subadditivity inequality is always satisfied in the AdS case, while the boosted strong subadditivity inequality is violated. This violation is consistent within the framework of $T\bar{T}$ -deformed theories, where the boundary field theory resides on a finitely truncated surface. In such scenarios, the entanglement wedge of the boosted subsystem A is not fully contained within the entanglement wedge of $A \cup B$ [78].

3.2 dS case

In the context of the dS spacetime, there are two primary holographic models: dS/CFT and dS/dS. The focus here is on the dS/dS correspondence in Euclidean signature, where the holographic boundary is a 2-dimensional sphere. The metric of the dS spacetime in global coordinates is given by

$$ds^2 = \ell_{\text{dS}}^2 \left[-dt^2 + \cosh^2 t (d\theta^2 + \sin^2 \theta d\phi^2) \right], \quad (3.18)$$

where the radius of the boundary sphere is $r = \ell_{\text{dS}} \cosh t$, which exceeds ℓ_{dS} for any finite cutoff at $t = t_c$. In dS/dS coordinates, the metric of the dS spacetime is

$$ds^2 = \ell_{\text{dS}}^2 [dw^2 + \sin^2 w (-d\tau^2 + \cosh^2 \tau d\phi^2)], \quad (3.19)$$

where the effective sphere radius is $r = \ell_{\text{dS}} \sin w < \ell_{\text{dS}}$. The point $r = \ell_{\text{dS}}$ corresponds to the cosmological horizon of the dS spacetime. When $r > \ell_{\text{dS}}$, the hypersurface $r = r_c$ is spacelike, which aligns with the standard dS/CFT duality. Conversely, when $r < \ell_{\text{dS}}$, the hypersurface $r = r_c$ becomes timelike, corresponding to the dS/dS correspondence, as illustrated in figure 5.

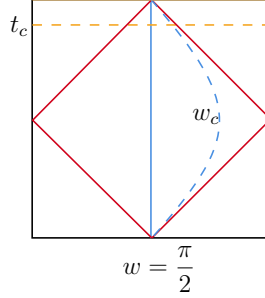


Figure 5. The Penrose diagram for the dS spacetime. The orange solid line represents future infinity, while the orange dashed line represents the finite cutoff at $t = t_c$. The red squares represent the boundaries at $w = 0, \pi$ in dS/dS coordinates. The blue solid line represents $w = \pi/2$, and the blue dashed line represents the finite cutoff at $w = w_c$.

For the dS/CFT duality, the assumed form of the quasi-local stress tensor (3.7) is substituted into eq. (2.19) to determine the value of α :

$$8\pi G \ell_{\text{dS}} \alpha^2 = 2i\alpha + \frac{\ell_{\text{dS}}}{16\pi G} \mathcal{R}^{(2)}, \quad \alpha = \frac{i}{\pi \lambda_{\text{dS}}} \left(1 - \sqrt{1 - \frac{\lambda_{\text{dS}} c_{\text{dS}}}{12r^2}} \right). \quad (3.20)$$

By integrating α with respect to r , the n -replica partition function is obtained as

$$\ln Z_n = -\frac{ic_{\text{dS}}}{3} \operatorname{arctanh} \left(\frac{1}{\sqrt{1 - \frac{c_{\text{dS}} \lambda_{\text{dS}}}{12r^2}}} \right) + \frac{i4r^2}{\lambda_{\text{dS}}} \left(-1 + \sqrt{1 - \frac{c_{\text{dS}} \lambda_{\text{dS}}}{12r^2}} \right). \quad (3.21)$$

The entanglement entropy between of A is then given by

$$S_A = \lim_{n \rightarrow 1} \left(1 - \frac{r}{2} \frac{d}{dr} \right) \ln Z_n = -\frac{ic_{\text{dS}}}{3} \operatorname{arctanh} \left(\frac{1}{\sqrt{1 - \frac{c_{\text{dS}} \lambda_{\text{dS}}}{12r^2}}} \right). \quad (3.22)$$

In this case, the argument of the inverse hyperbolic function is greater than one, making $\operatorname{arctanh} \left(\frac{1}{\sqrt{1 - \frac{c_{\text{dS}} \lambda_{\text{dS}}}{12r^2}}} \right)$ a complex value. The positive branch of the inverse hyperbolic function is chosen to match the real part of the entanglement entropy in the dS/CFT. The final

expression for the entanglement entropy in the dS/CFT correspondence is

$$S_A = -\frac{ic_{\text{dS}}}{3} \operatorname{arccoth} \left(\frac{1}{\sqrt{1 - \frac{c_{\text{dS}}\lambda_{\text{dS}}}{12r^2}}} \right) + \frac{\pi c_{\text{dS}}}{6}, \quad (3.23)$$

where the real part agrees with the results in refs. [25, 55, 79]. As discussed in ref. [52], the entanglement entropy in the dS/CFT can be interpreted as the pseudo entropy, which is viewed as the origin of the non-unitarity of the boundary field theory in the dS/CFT. Additionally, we still want to use the C -function to measure the degree of freedom of the field theory. However, due to the non-unitarity of the dual field theory, the C -function is also a purely imaginary number.

$$C(r) = 3rS'_A(r) = -ic_{\text{dS}} \frac{1}{\sqrt{1 - \frac{c_{\text{dS}}\lambda_{\text{dS}}}{12r^2}}}. \quad (3.24)$$

For the undeformed CFT, we have $C(r \rightarrow \infty) = -ic_{\text{dS}} = c$. But when $r \rightarrow \ell_{\text{dS}}$, the imaginary part of the C -function diverges, as shown in figure 6.

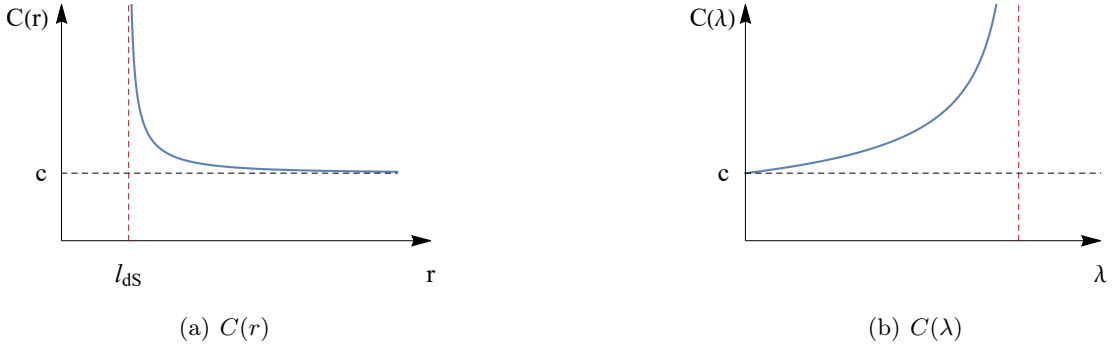


Figure 6. The C -function of the dS spacetime at $r > \ell_{\text{dS}}$, and $\lambda = \frac{\lambda_{\text{dS}}}{r^2}$. The red dashed line represents $r = \ell_{\text{dS}}$.

In the dS/dS case, the entanglement entropy and C -function have been analyzed in refs. [60, 66], with the results given as

$$S_A = \frac{c_{\text{dS}}}{3} \arctan \left(\frac{1}{\sqrt{\frac{c_{\text{dS}}\lambda_{\text{dS}}}{12r^2} - 1}} \right), \quad C(r) = 3rS'_A(r) = c_{\text{dS}} \frac{1}{\sqrt{\frac{c_{\text{dS}}\lambda_{\text{dS}}}{12r^2} - 1}}. \quad (3.25)$$

It is noted that when the effective radius is expressed as $r = \ell_{\text{dS}} \sin w < \ell_{\text{dS}}$, these results can be directly obtained through analytic continuation from the corresponding entanglement entropy and C -function in the dS/CFT correspondence. The C -function does decrease monotonically as r decreases, and it still diverges at $r = \ell_{\text{dS}}$, as shown in figure 7.

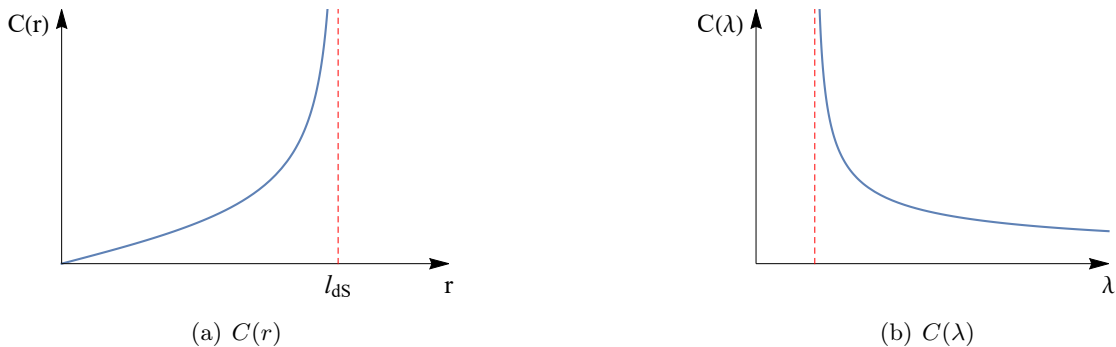


Figure 7. The C -function of the dS spacetime at $r < \ell_{\text{dS}}$.

By calculating the second derivative of the entanglement entropy with respect to the sphere radius r , it can be found that when the dual field theory resides on a timelike boundary, the entanglement entropy violates the strong subadditivity inequality,

$$r^2 \partial_r^2 S_A(r) = \frac{1}{\left(\frac{c_{\text{dS}} \lambda_{\text{dS}}}{12r^2} - 1\right)^{\frac{3}{2}}} > 0. \quad (3.26)$$

Therefore, it implies that the dual field theory is non-local [62, 65] when the effective radius of the sphere is smaller than the cosmological horizon.

4 Entanglement entropy for arbitrary single spatial intervals

In section 3, the replica method is employed to calculate the entanglement entropy for a subsystem between two antipodal points on a sphere under $T\bar{T}$ deformation. This method applies only to subsystems along semicircular arcs between antipodal points. To analyze the entanglement entropy for subsystems in arbitrary single spatial intervals on a two-dimensional plane, ref. [74] introduced the CHM mapping, which transforms the subsystem into a semicircular arc on a two-dimensional sphere. The entanglement entropy can then be determined using the results obtained for the spherical case. For subsystems on more general manifolds, they can first be mapped onto the two-dimensional plane, after which the method from ref. [74] can be applied. The replica method is generalized in the following section to calculate the entanglement entropy for arbitrary single spatial intervals on the two-dimensional plane with $T\bar{T}$ deformation and extended to general manifolds, including cylinders and spheres.

4.1 The generalization of the replica method

The goal is to calculate the entanglement entropy of the $T\bar{T}$ -deformed quantum field theory in a spatial subregion A on an arbitrary two-dimensional manifold \mathcal{M} , where A is defined by $t = 0$ and $x \in [x_a, x_b]$ in a chosen coordinate system. When \mathcal{M} is a two-dimensional sphere and A is specified by $\phi = \text{constant}$ and $\theta \in (0, \pi)$, the entanglement entropy can be computed using eqs. (3.4) and (3.5).

The entanglement entropy of A can be obtained through the C -function. Differentiating S_A with respect to r , we have

$$\begin{aligned}
r \frac{d}{dr} S_A(r) &= r \frac{d}{dr} \lim_{n \rightarrow 1} (1 - n \partial_n) \ln Z_n = \lim_{n \rightarrow 1} (1 - n \partial_n) r \frac{d}{dr} \ln Z_n \\
&= - \lim_{n \rightarrow 1} (1 - n \partial_n) 2\pi n r^2 \int_0^\pi \sin \theta d\theta \operatorname{tr} T \\
&= 2\pi r^2 \lim_{n \rightarrow 1} n^2 \int_0^\pi \sin \theta d\theta \partial_n \operatorname{tr} T,
\end{aligned} \tag{4.1}$$

where, in the last two steps, it is assumed that the metric (3.2) is independent of the azimuthal angle ϕ , and thus T_{ab} is also independent of ϕ . Solving the trace flow and conservation equations without assuming spherical symmetry must determine the energy-momentum tensor T_{ab} . For the n -replica sphere (3.2), the solution for the energy-momentum tensor is known [78] and is given by

$$\begin{aligned}
T^\theta_\theta &= \frac{1}{\pi \lambda} \left(1 - \sqrt{1 + \frac{\lambda c}{12r^2} + \frac{\lambda c}{12r^2} \left(\frac{1}{n^2} - 1 \right) \frac{1}{\sin^2 \theta}} \right), \\
T^\phi_\phi &= \frac{1}{\pi \lambda} \left(1 - \frac{1 + \frac{\lambda c}{12r^2}}{\sqrt{1 + \frac{\lambda c}{12r^2} + \frac{\lambda c}{12r^2} \left(\frac{1}{n^2} - 1 \right) \frac{1}{\sin^2 \theta}}} \right).
\end{aligned} \tag{4.2}$$

Substituting this into the integral in eq. (4.1), in the limit $n \rightarrow 1$, the integrand becomes

$$n \partial_n \operatorname{tr} T = \frac{c}{3} \frac{\lambda c}{48\pi} \frac{1 - n^2}{n^4 r^4 \sin^4 \theta} \frac{1}{\left[1 + \frac{\lambda c}{12r^2} \left(1 + \frac{2(1-n)}{\sin^2 \theta} \right) \right]^{3/2}}, \tag{4.3}$$

which tends to zero for $\theta \neq 0, \pi$. However, near the branch points, the integrand has a non-zero contribution. Thus, the main contribution to the integral in eq. (4.1) comes from small neighborhoods near the branch points

$$r S'(r) = 2\pi r^2 \lim_{n \rightarrow 1} \left(\int_{\theta \in B(0, \epsilon)} + \int_{\theta \in B(\pi, \epsilon)} \right) \sin \theta d\theta \partial_n \operatorname{tr} T, \tag{4.4}$$

where $B(p, \epsilon)$ is a small neighborhood centered at p with radius ϵ .

For a general manifold \mathcal{M} , we first map \mathcal{M} to \mathbb{S}^2 , ensuring that the image of the subsystem A under this mapping is a meridian on \mathbb{S}^2 . The mapped metric is conformally equivalent to the sphere, denoted as $\Omega \mathbb{S}^2$. After applying the n -replica trick, we assume the metric takes the form

$$ds^2 = r^2 \Omega^2(\theta, \phi) (d\theta^2 + n^2 \sin^2 \theta d\phi^2), \tag{4.5}$$

where the conformal factor $\Omega(\theta, \phi)$ is constant at the branch points $\theta = 0$ and $\theta = \pi$, denoted as Ω_0 and Ω_π , respectively. For this metric, eqs. (3.4) and (3.5) remain valid

$$\frac{d}{dr} \ln Z_n = - \int_{\Omega \mathbb{S}_n^2} d^2 x \frac{\delta \mathcal{L}}{\delta g_{ab}} \frac{dg_{ab}}{dr} = - \frac{1}{r} \int_{\Omega \mathbb{S}_n^2} d^2 x \sqrt{g} T^{ab} g_{ab}. \tag{4.6}$$

Thus, we have

$$\begin{aligned}
r \frac{d}{dr} S(r) &= r \frac{d}{dr} \lim_{n \rightarrow 1} (1 - n \partial_n) \ln Z_n = \lim_{n \rightarrow 1} (1 - n \partial_n) r \frac{d}{dr} \ln Z_n \\
&= - \lim_{n \rightarrow 1} (1 - n \partial_n) n r^2 \int_{\Omega \mathbb{S}_n^2} \Omega^2(\theta, \phi) \sin \theta d\theta d\phi \operatorname{tr} T \\
&= r^2 \lim_{n \rightarrow 1} n^2 \int_{\Omega \mathbb{S}_n^2} \Omega^2(\theta, \phi) \sin \theta d\theta d\phi \partial_n \operatorname{tr} T.
\end{aligned} \tag{4.7}$$

Since the conformal factor $\Omega(\theta, \phi)$ depends on the azimuthal angle ϕ , T_{ab} cannot be assumed to depend solely on θ . Therefore, the ϕ coordinate is not integrated in the final two steps. In standard CFT calculations, a conformal transformation is often applied to map $\Omega \mathbb{S}^2$ to the spherical metric, and conformal symmetry ensures that the results for $\Omega \mathbb{S}^2$ and \mathbb{S}^2 differ only by a function of the conformal factor. However, for the $T\bar{T}$ -deformed field theory, conformal symmetry is absent, and the relationship between quantities before and after the conformal transformation is not determined. As discussed in ref. [78], for the partition function on the sphere (4.1), in the limit $n \rightarrow 1$, the main contribution to the integral (4.1) comes from a small neighborhood near the branch points, with radius $\epsilon \sim \sqrt{n-1}$. This property is expected to hold for any manifold \mathcal{M} , so the integral (4.7) is also performed only in small neighborhoods near the branch points. In these regions, the conformal factor Ω is constant, and the metric (4.5) can be approximated by the n -replica sphere with radius $r\Omega$. As a result, the conformal transformation can be regarded as an identity transformation. Therefore, partition functions on any manifold \mathcal{M} can be calculated using the results on \mathbb{S}^2 for non-conformal field theories. Finally, we can get

$$\begin{aligned}
r S'(r) &= - \lim_{n \rightarrow 1} (1 - n \partial_n) \int_{\Omega \mathbb{S}_n^2} d^2 x \sqrt{g} \operatorname{tr} T \\
&= \lim_{n \rightarrow 1} 2\pi (r\Omega)^2 \left(\int_0^{\theta_0} + \int_{\pi-\theta_0}^{\pi} \right) \sin \theta d\theta \partial_n \operatorname{tr} T,
\end{aligned} \tag{4.8}$$

where $\operatorname{tr} T$ corresponds to the solution on the sphere with radius $r\Omega$.

When Poincaré coordinates are chosen in EAdS₃, the holographic boundary corresponds to a two-dimensional complex plane with the metric

$$ds_2^2 = \frac{\ell_{\text{AdS}}^2}{z_c^2} (dT^2 + dX^2). \tag{4.9}$$

The subregion A is defined by $T = 0$ and $X \in (-X_a, X_a)$. To compute the entanglement entropy for A , the complex plane is mapped onto a two-dimensional sphere such that the image of A corresponds to the meridian on the sphere at $\phi = 0$, as illustrated in figure 8. This mapping, known as the CHM mapping, is given by

$$X = \frac{X_a \cos \theta}{1 + \sin \theta \cos \phi}, \quad T = \frac{X_a \sin \theta \sin \phi}{1 + \sin \theta \cos \phi}. \tag{4.10}$$

Under this transformation, the boundary plane in (θ, ϕ) coordinates has the metric

$$ds_2^2 = \frac{\ell_{\text{AdS}}^2 X_a^2}{z_c^2 (1 + \cos \phi \sin \theta)^2} (d\theta^2 + \sin^2 \theta d\phi^2), \quad (4.11)$$

which is conformally equivalent to a sphere with an effective radius $r_{\text{eff}} = \frac{\ell_{\text{AdS}} X_a}{z_c}$, and the conformal factor $\Omega(\theta, \phi) = (1 + \cos \phi \sin \theta)^{-1}$.

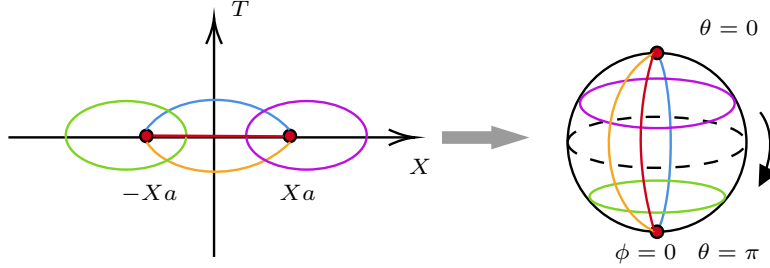


Figure 8. Mapping from the plane to the sphere. The north and south poles of the sphere correspond to the endpoints of the interval A on the complex plane. The subregion A corresponds to the meridian at $\phi = 0$, while the locally time-evolved subregions (shown as blue or yellow lines) correspond to other meridians on the sphere.

At this stage, the energy-momentum tensor for the metric (4.11) must be determined using the equations in (3.6), followed by evaluating the integral in (4.1). As previously noted, when computing the partition function on a general manifold \mathcal{M} , the primary contribution to the integral (4.1) comes from an infinitesimal neighborhood near the branch points. In these regions, the conformal factor $\Omega(\theta, \phi)$ can be approximated as 1, implying that the metric (4.11) effectively describes a sphere with radius $r_{\text{eff}} = \frac{\ell_{\text{AdS}} X_a}{z_c}$. Thus, within the infinitesimal neighborhoods around the endpoints, transforming (4.9) to the sphere involves only a conformal transformation with a conformal factor of 1, effectively an identity transformation. Consequently, the partition function remains the same as that of the sphere, with the radius r replaced by the effective radius r_{eff} .

For the AdS/CFT, the deformation parameter λ and the central charge c in eq. (3.6) are $c_{\text{AdS}} = \frac{3\ell_{\text{AdS}}}{2G}$ and $\lambda_{\text{AdS}} = 8G\ell_{\text{AdS}}$, respectively. Therefore, the solution for the energy-momentum tensor on the n -replica sphere is

$$\begin{aligned} T^\theta_\theta &= \frac{1}{\pi\lambda_{\text{AdS}}} \left(1 - \sqrt{1 + \frac{\lambda_{\text{AdS}} c_{\text{AdS}}}{12r_{\text{eff}}^2} + \frac{\lambda_{\text{AdS}} c_{\text{AdS}}}{12r_{\text{eff}}^2} \left(\frac{1}{n^2} - 1 \right) \frac{1}{\sin^2 \theta}} \right), \\ T^\phi_\phi &= \frac{1}{\pi\lambda_{\text{AdS}}} \left(1 - \frac{1 + \frac{\lambda_{\text{AdS}} c_{\text{AdS}}}{12r_{\text{eff}}^2}}{\sqrt{1 + \frac{\lambda_{\text{AdS}} c_{\text{AdS}}}{12r_{\text{eff}}^2} + \frac{\lambda_{\text{AdS}} c_{\text{AdS}}}{12r_{\text{eff}}^2} \left(\frac{1}{n^2} - 1 \right) \frac{1}{\sin^2 \theta}}} \right), \end{aligned} \quad (4.12)$$

where the effective radius is $r_{\text{eff}} = \frac{\ell_{\text{AdS}} X_a}{z_c}$. Substituting this into eq. (4.1) and performing the

integration near the endpoints yields the C -function as

$$C(r) = \frac{c_{\text{AdS}}}{3} \frac{1}{\sqrt{1 + \frac{c_{\text{AdS}}\lambda_{\text{AdS}}}{12r_{\text{eff}}^2}}}. \quad (4.13)$$

Using the C -function, one can get the entanglement entropy of the subregion A as

$$S_A = \frac{c_{\text{AdS}}}{3} \operatorname{arctanh} \left(\frac{1}{\sqrt{1 + \frac{c_{\text{AdS}}\lambda_{\text{AdS}}}{12r_{\text{eff}}^2}}} \right) \simeq \frac{c_{\text{AdS}}}{3} \log \frac{2X_a}{z_c} + \frac{c_{\text{AdS}}}{12} \frac{z_c^2}{X_a^2}. \quad (4.14)$$

In this expression, the first term represents the entanglement entropy of the undeformed field theory in the interval $(-X_a, X_a)$ on the plane. The second term accounts for the correction introduced by the $T\bar{T}$ deformation. This result is consistent with the findings reported in ref. [21].

For the dS/CFT, the deformation parameter λ and the central charge c in eq. (3.6) are given by $c \equiv -ic_{\text{dS}} = -i\frac{3\ell_{\text{dS}}}{2G}$ and $\lambda \equiv -i\lambda_{\text{dS}} = -i8G\ell_{\text{dS}}$, respectively. The solution for the energy-momentum tensor on the n -replica sphere

$$\begin{aligned} T^\theta_\theta &= \frac{i}{\pi\lambda_{\text{dS}}} \left(1 - \sqrt{1 - \frac{\lambda_{\text{dS}}c_{\text{dS}}}{12r_{\text{eff}}^2} - \frac{\lambda_{\text{dS}}c_{\text{dS}}}{12r_{\text{eff}}^2} \left(\frac{1}{n^2} - 1 \right) \frac{1}{\sin^2\theta}} \right), \\ T^\phi_\phi &= \frac{i}{\pi\lambda_{\text{dS}}} \left(1 - \frac{1 - \frac{\lambda_{\text{dS}}c_{\text{dS}}}{12r_{\text{eff}}^2}}{\sqrt{1 - \frac{\lambda_{\text{dS}}c_{\text{dS}}}{12r_{\text{eff}}^2} - \frac{\lambda_{\text{dS}}c_{\text{dS}}}{12r_{\text{eff}}^2} \left(\frac{1}{n^2} - 1 \right) \frac{1}{\sin^2\theta}}} \right), \end{aligned} \quad (4.15)$$

where the effective radius is $r_{\text{eff}} = \frac{\ell_{\text{dS}}X_a}{\eta_c}$. Substituting this into eq. (4.1), we obtain the C -function is

$$C(r) = -\frac{ic_{\text{dS}}}{3} \frac{1}{\sqrt{1 - \frac{c_{\text{dS}}\lambda_{\text{dS}}}{12r_{\text{eff}}^2}}}. \quad (4.16)$$

The entanglement entropy is then given by

$$S_A = -\frac{ic_{\text{dS}}}{3} \operatorname{arccoth} \left(\frac{1}{\sqrt{1 - \frac{c_{\text{dS}}\lambda_{\text{dS}}}{12r_{\text{eff}}^2}}} \right) + \frac{\pi c_{\text{dS}}}{6} \simeq -\frac{ic_{\text{dS}}}{3} \log \frac{2X_a}{\eta_c} + \frac{ic_{\text{dS}}\eta_c^2}{12X_a^2} + \frac{\pi c_{\text{dS}}}{6}. \quad (4.17)$$

In Appendix A.1, this quantity is computed using holographic methods by evaluating the area of the RT surface with a finite cutoff η_c . The result is consistent with eq. (4.17).

To generalize the method for computing subsystems' entanglement entropy on arbitrary holographic boundaries, we note that any two-dimensional manifold is locally conformally equivalent to the plane. Thus, its line element can be expressed as

$$ds^2 = \omega(T, X)^2 (dT^2 + dX^2). \quad (4.18)$$

Suppose the subregion A in the coordinate system (T, X) is a line segment with endpoints at $(T_a, -X_a)$ and (T_a, X_a) . To calculate the entanglement entropy of this subsystem, we map it onto the sphere using the transformation

$$T \rightarrow \frac{X_a \sin \theta \sin \phi}{1 + \sin \theta \cos \phi} + T_a, \quad X \rightarrow \frac{X_a \cos \theta}{1 + \sin \theta \cos \phi}. \quad (4.19)$$

This mapping sends the endpoints $(T_a, -X_a)$ and (T_a, X_a) on the plane to the antipodal points on the sphere. The line element (4.18) in these new coordinates becomes

$$ds^2 = \frac{\omega(T(\theta, \phi), X(\theta, \phi))^2 X_a^2}{(1 + \cos \phi \sin \theta)^2} (d\theta^2 + \sin^2 \theta d\phi^2), \quad (4.20)$$

where $\theta(T_a, X_a) = 0$ and $\theta(T_a, -X_a) = \pi$. We then perform a conformal transformation to eliminate the conformal factor $\frac{\omega(T(\theta, \phi), X(\theta, \phi))}{1 + \cos \phi \sin \theta}$, resulting in a sphere with an effective radius r_{eff} . If $\omega(T(\theta, \phi), X(\theta, \phi))$ is constant at both endpoints, this factor only contributes to the effective radius. At the endpoints $\theta = 0$ and π , the factor $1 + \cos \phi \sin \theta$ is 1. Thus, near these endpoints, the metric (4.20) approximates that of a sphere, with an effective radius of $\omega(T_a, X_a)X_a$. Once again, assuming that the integrand in (4.1) is non-zero only in small neighborhoods near the endpoints, the conformal transformation is the identity map in these neighborhoods. Thus, we can directly use the partition function on the sphere with radius r_{eff} as the partition function on the manifold \mathcal{M} within the subregion A . Within these small neighborhoods, we can use the solution for the energy-momentum tensor on the n -sphere to compute the integral, with the effective radius in the solutions (4.12) or (4.15) replaced by $r_{\text{eff}} = \omega(T_a, X_a)X_a$.

If $\omega(T, X)$ takes different constant values at the two endpoints, denoted as ω_a and ω_{-a} , respectively. The contributions to the integral (4.1) from different endpoints correspond to spheres with radii $\omega_a X_a$ and $\omega_{-a} X_a$. Therefore, these integrals should be replaced by the partition function on spheres with radii $\omega_a X_a$ and $\omega_{-a} X_a$, respectively.

4.2 System with finite size

In the previous subsection, we reviewed the CHM mapping method for calculating the entanglement entropy of the $T\bar{T}$ -deformed CFT in spatial intervals on a two-dimensional plane. Specifically, we computed the entanglement entropy for a subsystem on the boundary of the dS spacetime in Poincaré coordinates. We now extend this method to two-dimensional cylindrical and spherical surfaces to examine whether the $T\bar{T}$ deformation introduces corrections to the entanglement entropy for finite-size systems. The corresponding holographic models for these geometries are AdS and dS spacetimes in global coordinates, respectively. The entanglement entropy calculation for general spatial intervals in curved space has been discussed in ref. [92].

4.2.1 AdS case

The metric of EAdS₃ in global coordinates is

$$ds_{\text{EAdS}_3}^2 = \ell_{\text{AdS}}^2 (d\rho^2 + \cosh^2 \rho dt^2 + \sinh^2 \rho dx^2), \quad (4.21)$$

where $x \sim x + 2\pi$. At the boundary $\rho = \rho_c$, we can get the induced metric as

$$ds_{\text{cyl}}^2 = \ell_{\text{AdS}}^2 \sinh^2 \rho_c (d\tilde{t}^2 + dx^2), \quad (4.22)$$

where $\tilde{t} = \frac{\cosh \rho_c}{\sinh \rho_c} t$. To compute the entanglement entropy of a subsystem in the subregion A defined by the interval $(-x_a, x_a)$ on the time slice $t = 0$, we first map the cylinder onto the complex plane using the following transformations

$$\tilde{t} \rightarrow \frac{1}{2} \ln(T^2 + X^2), \quad x \rightarrow \frac{1}{2i} \ln \left(\frac{T + iX}{T - iX} \right). \quad (4.23)$$

Under this transformation, the endpoints $(0, -x_a)$ and $(0, x_a)$ of A are mapped to $(T_a, -X_a) = (\cos x_a, -\sin x_a)$ and $(T_a, X_a) = (\cos x_a, \sin x_a)$, respectively. The line element in this coordinate becomes

$$ds_{\text{pl}}^2 = \ell_{\text{AdS}}^2 \sinh^2 \rho_c \frac{dT^2 + dX^2}{T^2 + X^2}. \quad (4.24)$$

Next, we apply the CHM transformation to map the plane onto a two-dimensional sphere, with the coordinate transformation

$$T \rightarrow \frac{\sin x_a \sin \theta \sin \phi}{1 + \sin \theta \cos \phi} + \cos x_a, \quad X \rightarrow \frac{\sin x_a \cos \theta}{1 + \sin \theta \cos \phi}. \quad (4.25)$$

This transformation maps the endpoints of the interval on the plane to antipodal points on the sphere. In these new coordinates, the metric becomes

$$\begin{aligned} ds_{\Omega\text{S}^2}^2 &= \frac{\ell_{\text{AdS}}^2 \sinh^2 \rho_c \sin^2 x_a}{(1 + \cos(2x_a - \phi) \sin \theta)(1 + \cos \phi \sin \theta)} (d\theta^2 + \sin^2 \theta d\phi^2) \\ &= \Omega^2(\theta, \phi) r_{\text{eff}}^2 (d\theta^2 + \sin^2 \theta d\phi^2), \end{aligned} \quad (4.26)$$

where the effective radius is $r_{\text{eff}} = \ell_{\text{AdS}} \sinh \rho_c \sin x_a$, and the conformal factor is $\Omega^{-2}(\theta, \phi) = (1 + \cos(2x_a - \phi) \sin \theta)(1 + \cos \phi \sin \theta)$. The mapping from the cylinder to the sphere is illustrated in figure 9.

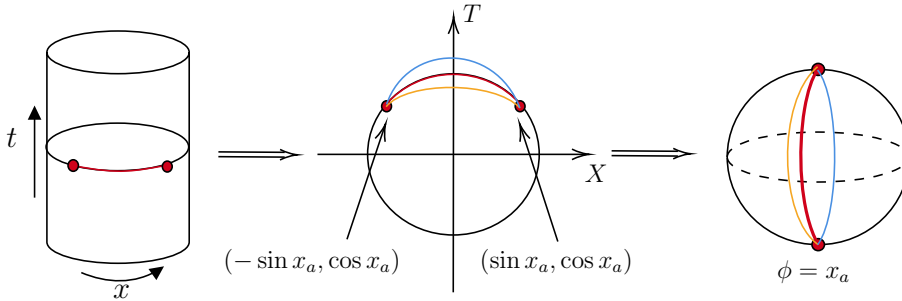


Figure 9. The CHM transformation for the AdS case. After applying two mappings, an arc on the cylinder with endpoints $(-x_a, x_a)$ is mapped to a meridian on the sphere at $\phi = x_a$. The meridian is then replicated n times by cutting it along the ϕ direction. Using the replica trick, the entanglement entropy of the subregion A is calculated.

At the antipodal points $\theta = 0, \pi$, the conformal factor simplifies to $\Omega = 1$, allowing us to directly compute the entanglement entropy. The resulting entanglement entropy for the subregion A is given by

$$S_A = \frac{c_{\text{AdS}}}{3} \operatorname{arctanh} \left(\frac{1}{\sqrt{1 + \frac{c_{\text{AdS}} \lambda_{\text{AdS}}}{12 r_{\text{eff}}^2}}} \right) \simeq \frac{c_{\text{AdS}}}{3} \log(2 \sinh \rho_c \sin x_a) + \frac{c_{\text{AdS}}}{12 \sinh^2 \rho_c \sin^2 x_a}, \quad (4.27)$$

where the first term of the last line represents the entanglement entropy of the undeformed field theory for the interval $(-x_a, x_a)$ on the cylinder, with the UV cutoff $\epsilon = \frac{1}{2 \sinh \rho_c}$. The second term accounts for the contribution from the $T\bar{T}$ deformation. This expression aligns with the perturbative results found in ref. [16].

4.2.2 dS case

For the global coordinates of the dS spacetime, the metric is given by

$$ds^2 = \ell_{\text{dS}}^2 (-dt^2 + \cosh^2 t (d\Theta^2 + \sin^2 \Theta d\Phi^2)). \quad (4.28)$$

After the $T\bar{T}$ deformation, its holographic boundary is a 2-dimensional sphere determined by $t = t_c$. The subregion A is defined by the arc $\Theta = \pi/2$, $\Phi \in (-\Phi_a, \Phi_a)$ on this 2-dimensional sphere. As done previously, we begin by mapping the sphere to the complex plane using the transformation

$$\Theta = 2 \arctan \sqrt{T^2 + X^2}, \quad \Phi = \frac{1}{2i} \ln \frac{T + iX}{T - iX}. \quad (4.29)$$

In this coordinate system, the endpoints of A are $(\cos \Phi_a, -\sin \Phi_a)$ and $(\cos \Phi_a, \sin \Phi_a)$, and the line element becomes

$$ds^2 = \frac{4\ell_{\text{dS}}^2 \cosh^2 t_c}{1 + X^2 + T^2} (dT^2 + dX^2). \quad (4.30)$$

As shown in figure 10, after the above mapping, we map an arc on the sphere to an arc on the plane. We then apply the CHM transformation

$$T \rightarrow \frac{\sin \Phi_a \sin \theta \sin \phi}{1 + \sin \theta \cos \phi} + \cos \Phi_a, \quad X \rightarrow \frac{\sin \Phi_a \cos \theta}{1 + \sin \theta \cos \phi}, \quad (4.31)$$

which maps this subregion to the meridian $\phi = \Phi_a$ on the sphere.

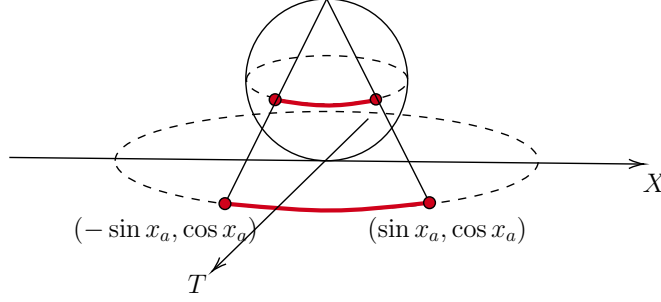


Figure 10. The CHM transformation of the global dS case.

The transformed line element is

$$\begin{aligned} ds^2 &= \frac{\ell_{\text{dS}}^2 \cosh^2 t_c \sin^2 \Phi_a}{(1 + \cos(\phi - \Phi_a) \cos(\Phi_a) \sin(\theta))^2} (d\theta^2 + \sin^2 \theta d\phi^2) \\ &= \Omega(\theta, \phi)^2 r_{\text{eff}}^2 (d\theta^2 + \sin^2 \theta d\phi^2), \end{aligned} \quad (4.32)$$

where $r_{\text{eff}} = \ell_{\text{dS}} \cosh t_c \sin \Phi_a$ is the effective radius of the sphere, and the conformal factor is

$$\Omega(\theta, \phi) = \frac{1}{1 + \cos(\phi - \Phi_a) \cos(\Phi_a) \sin(\theta)}. \quad (4.33)$$

At the antipodal points $\theta = 0, \pi$, the conformal factor $\Omega(\theta, \phi) = 1$, allowing us to directly use the results in eq. (4.15) to calculate the entanglement entropy. The final result is

$$\begin{aligned} S_A &= -\frac{ic_{\text{dS}}}{3} \operatorname{arccoth} \left(\frac{1}{\sqrt{1 - \frac{c_{\text{dS}} \lambda_{\text{dS}}}{12r_{\text{eff}}^2}}} \right) + \frac{\pi c_{\text{dS}}}{6} \\ &\simeq -\frac{ic_{\text{dS}}}{3} \log(2 \cosh t_c \sin \Phi_a) + \frac{ic_{\text{dS}}}{12 \cosh^2 t_c \sin^2 \Phi_a} + \frac{\pi c_{\text{dS}}}{6}. \end{aligned} \quad (4.34)$$

This result is consistent with the area of the RT surface calculated in Appendix A.2, and also matches the findings of ref. [79] when $\Phi_a = \frac{\pi}{2}$.

4.3 System with finite temperature

In ref. [16], the authors mentioned that entanglement entropy receives a first-order correction from the $T\bar{T}$ deformation only for the finite temperature case. Thus, in this subsection, we focus on investigating the entanglement entropy of the planar Bañados-Teitelboim-Zanelli (BTZ) [105] black hole. For the Euclidean BTZ black hole, the bulk metric is given by

$$ds^2 = \frac{R^2 - R_0^2}{\ell_{\text{AdS}}^2} dt^2 + \frac{\ell_{\text{AdS}}^2}{R^2 - R_0^2} dR^2 + R^2 dx^2, \quad (4.35)$$

where x is the coordinate of the non-compact direction, and t is periodic with $t \sim t + \beta$, where $\beta = \frac{2\pi\ell_{\text{AdS}}^2}{R_0}$ is the inverse Hawking temperature. The induced metric on the holographic

boundary $R = R_c$ is

$$ds^2 = \frac{R_c^2 - R_0^2}{\ell_{\text{AdS}}^2} \left(dt^2 + \frac{R_c^2 \ell_{\text{AdS}}^2}{R_c^2 - R_0^2} dx^2 \right) := \frac{R_c^2 - R_0^2}{\ell_{\text{AdS}}^2} (dt^2 + d\tilde{x}^2), \quad (4.36)$$

where $\tilde{x} = \frac{R_c \ell_{\text{AdS}}}{\sqrt{R_c^2 - R_0^2}} x$. We aim to compute the entanglement entropy of the subsystem within the interval $x \in (-x_a, x_a)$ at $t = 0$. The length of the interval is $L = \frac{2x_a R_c \ell_{\text{AdS}}}{\sqrt{R_c^2 - R_0^2}}$. To simplify the calculation, we redefine the coordinates by

$$R = R_0 \cosh \rho, \quad t = \frac{\ell_{\text{AdS}}^2}{R_0} \phi = \frac{\beta}{2\pi} \phi, \quad x = \frac{\ell_{\text{AdS}}}{R_0} \tau \quad (4.37)$$

to transform the metric (4.35) to the global coordinate of EAdS₃

$$ds^2 = \ell_{\text{AdS}}^2 (\sinh^2 \rho d\phi^2 + d\rho^2 + \cosh^2 \rho d\tau^2). \quad (4.38)$$

At this point, the chosen subregion corresponds to the interval $\tau \in (-\tau_a, \tau_a)$ at $\phi = 0$, where $\tau_a = \frac{R_0}{\ell_{\text{AdS}}} x_a$. The holographic boundary $R = R_c$ corresponds to $\rho = \rho_c$ with $\cosh \rho_c = \frac{R_c}{R_0}$. The induced metric on this boundary is

$$ds^2 = \ell_{\text{AdS}}^2 \cosh^2 \rho_c (d\tau^2 + d\phi^2). \quad (4.39)$$

Up to this point, the setup remains similar to that in sec 4.2.1. According to eq. (4.23), the endpoints of the interval in the complex plane are $(T, X) = (e^{-\tau_a}, 0)$ and $(e^{\tau_a}, 0)$, and the line element in this coordinate becomes

$$ds_{\text{pl}}^2 = \ell_{\text{AdS}}^2 \cosh^2 \rho_c \frac{dT^2 + dX^2}{T^2 + X^2}. \quad (4.40)$$

For the interval $X = 0$, with $T_a \in (e^{-\tau_a}, e^{\tau_a})$, the CHM map takes the form

$$X \rightarrow \frac{\sinh \tau_a \sin \theta \sin \phi}{1 + \sin \theta \cos \phi}, \quad T \rightarrow \frac{\sinh \tau_a \cos \theta}{1 + \sin \theta \cos \phi} + \cosh \tau_a. \quad (4.41)$$

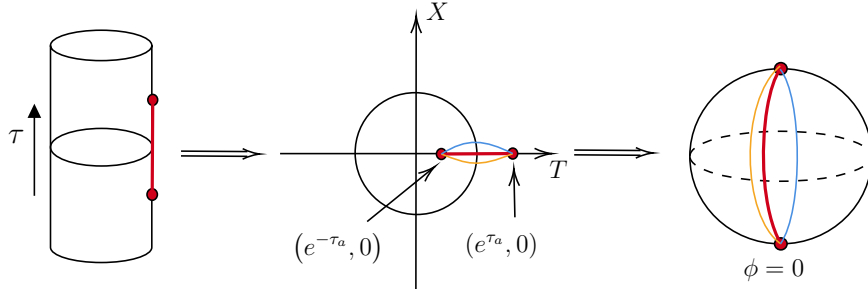


Figure 11. The CHM transformation of the BTZ black hole. In this case, the effective radius at the two endpoints is different.

As depicted in figure 11, under the CHM transformation, the interval along the cylindrical axis is mapped to the meridian at $\phi = 0$ on the sphere. The resulting metric in these coordinates is given by

$$ds^2 = \frac{\ell_{\text{AdS}}^2 \cosh^2 \rho_c \sinh^2 \tau_a (d\theta^2 + \sin^2 \theta d\phi^2)}{(1 + \cos \phi \sin \theta)(\cosh 2\tau_a + \cos \phi \sin \theta + \cos \theta \sinh 2\tau_a)}. \quad (4.42)$$

In contrast to the previous situation, the effective radius r_{eff} at the endpoints $\theta = 0$ and $\theta = \pi$ is not equal. We can regard the constant factor $\ell_{\text{AdS}} \cosh \rho_c \sinh \tau_a$ in the metric (4.42) as the role of radius “ r ” in eq. (4.7), with the remaining angle-dependent part serving as the conformal factor $\Omega(\theta, \phi)$. Accordingly, the effective radii corresponding to the two endpoints are

$$r_{\text{eff}, \theta=0} = r\Omega(0, \phi) = \ell_{\text{AdS}} \cosh \rho_c \sinh \tau_a e^{-2\tau_a} = \ell_{\text{AdS}} \frac{R_c}{R_0} e^{-\frac{2\pi L \sqrt{1 - \left(\frac{R_0}{R_c}\right)^2}}{\beta}} \sinh \frac{\pi L \sqrt{1 - \left(\frac{R_0}{R_c}\right)^2}}{\beta},$$

$$r_{\text{eff}, \theta=\pi} = r\Omega(\pi, \phi) = \ell_{\text{AdS}} \cosh \rho_c \sinh \tau_a e^{2\tau_a} = \ell_{\text{AdS}} \frac{R_c}{R_0} e^{\frac{2\pi L \sqrt{1 - \left(\frac{R_0}{R_c}\right)^2}}{\beta}} \sinh \frac{\pi L \sqrt{1 - \left(\frac{R_0}{R_c}\right)^2}}{\beta}. \quad (4.43)$$

As discussed at the end of Section 4.1, we assume that the CHM mapping method is still applicable. However, the energy-momentum tensor in the integrals near different endpoints corresponds to solutions on the sphere with different radii. According to eq. (4.8), we have

$$r \frac{d}{dr} S_A(r) = - \lim_{n \rightarrow 1} 2\pi \left[r^2 \Omega^2(0, \phi) \int_0^{\theta_0} \sin \theta d\theta \partial_n \text{Tr} T + r^2 \Omega^2(\pi, \phi) \int_{\pi - \theta_0}^{\pi} \sin \theta d\theta \partial_n \text{Tr} T \right]$$

$$= \frac{c}{6} \left(\frac{1}{\sqrt{1 + \frac{c_{\text{AdS}} \lambda_{\text{AdS}}}{12r^2 \Omega^2(0, \phi)}}} + \frac{1}{\sqrt{1 + \frac{c_{\text{AdS}} \lambda_{\text{AdS}}}{12r^2 \Omega^2(\pi, \phi)}}} \right). \quad (4.44)$$

Integrating the above function with respect to r , the entanglement entropy is given by

$$S_A = \frac{c_{\text{AdS}}}{6} \left[\text{arctanh} \left(\frac{1}{\sqrt{1 + \frac{c_{\text{AdS}} \lambda_{\text{AdS}}}{12r_{\text{eff}, \theta=0}^2}}} \right) + \text{arctanh} \left(\frac{1}{\sqrt{1 + \frac{c_{\text{AdS}} \lambda_{\text{AdS}}}{12r_{\text{eff}, \theta=\pi}^2}}} \right) \right]. \quad (4.45)$$

Substituting the radii $r_{\text{eff}, \theta}$ into this expression and expanding the result to second order in R_0/R_c ,

$$S_A \simeq \frac{c_{\text{AdS}}}{3} \left[\ln \left(\frac{\beta R_c \sinh \frac{\pi L}{\beta}}{\pi \ell_{\text{AdS}}^2} \right) - \frac{2\pi^3 \ell_{\text{AdS}}^4 L \coth \left(\frac{\pi L}{\beta} \right)}{R_c^2 \beta^3} + \frac{\pi^2 \ell_{\text{AdS}}^4 \left(1 + \coth \left(\frac{2\pi L}{\beta} \right) \right)}{R_c^2 \beta^2} \right], \quad (4.46)$$

where we have replaced R_0 with $\frac{2\pi \ell_{\text{AdS}}^2}{\beta}$. In the high-temperature limit $\beta \ll 1$, the last term is negligible compared to the second term. This result is consistent with the findings in refs. [16, 22] by identifying $R_c^2 = \frac{6\ell_{\text{AdS}}^2}{\mu\pi c_{\text{AdS}}}$.

5 (A)dS/dS case and non-locality

In this section, we apply the methods from the previous section to the AdS/dS, dS/dS, and half-dS holography cases. For all three, the holographic boundary is a timelike hypersurface. In dS/dS and half-dS holography, previous studies [62, 65] suggest that the dual field theory may exhibit non-locality. Unlike the examples discussed earlier, the boundary-induced metrics in this section are time-dependent. As a result, the properties of entanglement entropy may vary significantly over time, potentially influencing the determination of the strong subadditivity or the boosted strong subadditivity. This issue will be discussed in detail in this section.

5.1 AdS/dS

For the AdS/dS correspondence, the bulk metric is expressed as

$$ds^2 = \ell_{\text{AdS}}^2 (dw^2 + \sinh^2 w (-dt^2 + \cosh^2 t dx^2)), \quad (5.1)$$

where $x \sim x + 2\pi$, and the holographic boundary is determined by $w = w_c \rightarrow \infty$. We choose the boundary subregion A as $x \in (-x_a, x_a)$ at $t = t_0$. In the Euclidean signature, after rescaling the time coordinate, the boundary metric can be written as

$$ds^2 = \ell_{\text{AdS}}^2 \frac{\sinh^2 w_c}{\cosh^2 \tilde{t}} (d\tilde{t}^2 + dx^2), \quad (5.2)$$

where \tilde{t} is related to t by the relation

$$\tilde{t} = \ln \frac{\cot \frac{t}{2} + 1}{\cot \frac{t}{2} - 1}. \quad (5.3)$$

This metric is conformally equivalent to the cylinder. As we have done in the last section, we can map it to the complex plane through the following transformations

$$\tilde{t} \rightarrow \frac{1}{2} \ln(T^2 + X^2), \quad x \rightarrow \frac{1}{2i} \ln \left(\frac{T + iX}{T - iX} \right). \quad (5.4)$$

and the resulting conformal flat metric is

$$ds^2 = \ell_{\text{AdS}}^2 \sinh^2 w_c \frac{4(dT^2 + dX^2)}{(1 + T^2 + X^2)^2}. \quad (5.5)$$

The two endpoints of the subregion A in the (T, X) coordinates are

$$(T_1, X_1) = (e^{\tilde{t}_0} \cos x_a, -e^{\tilde{t}_0} \sin x_a), \quad (T_2, X_2) = (e^{\tilde{t}_0} \cos x_a, e^{\tilde{t}_0} \sin x_a). \quad (5.6)$$

Using the CHM map,

$$T \rightarrow \frac{e^{\tilde{t}_0} \sin x_a \sin \theta \sin \phi}{1 + \sin \theta \cos \phi} + e^{\tilde{t}_0} \cos x_a, \quad X \rightarrow \frac{e^{\tilde{t}_0} \sin x_a \cos \theta}{1 + \sin \theta \cos \phi}, \quad (5.7)$$

this complex plane can be mapped onto the sphere, yielding the conformal spherical metric

$$ds^2 = \frac{4e^{2\tilde{t}_0}\ell_{\text{AdS}}^2 \sinh^2 w_c \sin^2 x_a (d\theta^2 + \sin^2 \theta d\phi^2)}{(1 + \sin \theta \cos \phi + e^{2\tilde{t}_0} \sin \theta \cos(\phi - 2x_a) + e^{2\tilde{t}_0})^2}. \quad (5.8)$$

It is easy to verify that the conformal factor at the endpoints $\theta = 0, \pi$ is the same constant, which can be absorbed into r_{eff} . Therefore, the effective radius is

$$r_{\text{eff}} = \ell_{\text{AdS}} \sinh w_c \cos t_0 \sin x_a, \quad (5.9)$$

or, in Lorentz signature, $r_{\text{eff}} = \ell_{\text{AdS}} \sinh w_c \cosh t_0 \sin x_a$. Finally, the entanglement entropy of the subsystem is

$$S_A \simeq \frac{c_{\text{AdS}}}{3} \log(2 \sinh w_c \cosh t_0 \sin x_a) + \frac{c_{\text{AdS}}}{12 \sinh^2 w_c \cosh^2 t_0 \sin^2 x_a}. \quad (5.10)$$

If we choose the UV cutoff as $\sinh w_c = 1/\epsilon$, we find that eq.(5.10) agrees with the result in ref. [65]. Alternatively, if we select the subregion as $t = t_0$, $x \in [-\frac{\pi}{2}, \frac{\pi}{2}]$, the entanglement entropy is $S \simeq \frac{c_{\text{AdS}}}{3} w_c$, which matches the result in ref. [72]. For verification, we holographically calculate the area of the RT surface, which is expressed as

$$\begin{aligned} D_{12} &= \ell_{\text{AdS}} \text{arccosh}(1 + 2 \sinh^2 w_c \cosh^2 t_0 \sin^2 x) \\ &\simeq 2\ell_{\text{AdS}} \log(2 \sinh w_c \cosh t_0 \sin x_a) + \frac{\ell_{\text{AdS}}}{2 \sinh^2 w_c \cosh^2 t_0 \sin^2 x_a}. \end{aligned} \quad (5.11)$$

After dividing D_{12} by $4G$ and substituting the relation $G = 3\ell_{\text{AdS}}/2c_{\text{AdS}}$, it is consistent with (5.10) up to the second-order correction of the $T\bar{T}$ deformation.

5.2 dS/dS

For the dS/dS correspondence, the bulk metric is given by

$$ds^2 = \ell_{\text{dS}}^2 (dw^2 + \sin^2 w (-dt^2 + \cosh^2 t d\phi^2)), \quad (5.12)$$

with the holographic boundary specified at $w = w_c$. The subregion A is chosen as $t = t_0$, $\phi \in (-\phi_a, \phi_a)$. The boundary induced metric is

$$ds^2 = \ell_{\text{dS}}^2 \sin^2 w_c (-dt^2 + \cosh^2 t d\phi^2). \quad (5.13)$$

Comparing this with the metric in eq. (5.1), the only difference between the induced metrics for the dS and AdS cases is the replacement of the conformal factor $\sinh^2 w$ with $\sin^2 w$. As a result, the subsequent calculations are identical to those in the AdS case, except for replacing $\sinh^2 w_c$ with $\sin^2 w_c$. Consequently, the effective radius is given by $r_{\text{eff}} = \ell_{\text{dS}} \sin w_c \cosh t_0 \sin \phi_a$. For dS/dS, the entanglement entropy expression for a general spatial interval is given by eq. (3.25). In this case, the effective radius must be less than ℓ_{dS} , which implies

$$\sin w_c \cosh t_0 \sin \phi_a < 1. \quad (5.14)$$

Finally, we can obtain the entanglement entropy of subregion A as

$$S_A = \frac{c_{\text{dS}}}{3} \arctan \left(\frac{1}{\sqrt{\frac{c_{\text{dS}} \lambda_{\text{dS}}}{12 r_{\text{eff}}^2} - 1}} \right) = \frac{c_{\text{dS}}}{3} \arctan \left(\frac{1}{\sqrt{\frac{1}{(\sin w_c \cosh t_0 \sin \phi_a)^2} - 1}} \right). \quad (5.15)$$

For the specific case $t = 0$, we can derive the relation

$$\frac{1}{(\sin w_c \sin \phi_a)^2} - 1 = \cot^2 \phi_a + \frac{\cot^2 w_c}{\sin^2 \phi_a}. \quad (5.16)$$

Substituting this into (5.15), the entanglement entropy at $t_0 = 0$ becomes

$$S_A = \frac{c_{\text{dS}}}{3} \operatorname{arccot} \left(\sqrt{\cot^2 \phi_a + \frac{\cot^2 w_c}{\sin^2 \phi_a}} \right), \quad (5.17)$$

which is consistent with the holographic calculation of the area of the RT surface in ref. [62]. For the case where the subsystem is defined as $\phi \in (-\frac{\pi}{2}, \frac{\pi}{2})$, the entanglement entropy is given by $S_A = \frac{c_{\text{dS}}}{3} w_c$, which agrees with the result in ref. [66].

The next task is to determine whether the system's entanglement entropy satisfies the strong subadditivity inequality. To achieve this, we compute the second-order derivative of the entanglement entropy with respect to the subsystem scale $\Delta\phi$, where $\Delta\phi = 2\phi_a$. The result is

$$\partial_{\Delta\phi}^2 S_A(\Delta\phi) = -\frac{c_{\text{dS}}}{12 \sin^2 \frac{\Delta\phi}{2}} \frac{\frac{1}{\sin^2 w_c \cosh^2 t_0} - 1}{\left(\frac{1}{\sin^2 \frac{\Delta\phi}{2} \sin^2 w_c \cosh^2 t_0} - 1 \right)^{3/2}}. \quad (5.18)$$

We find that when $\sin w_c \cosh t_0 > 1$, the entanglement entropy always violates the strong subadditivity inequality. However, when $\sin w_c \cosh t_0 < 1$, for any $\Delta\phi$, the condition $r_{\text{eff}} < \ell_{\text{dS}}$ is always satisfied, and the entanglement entropy satisfies the strong subadditivity inequality, as illustrated in figure 12(a) and figure 12(b).

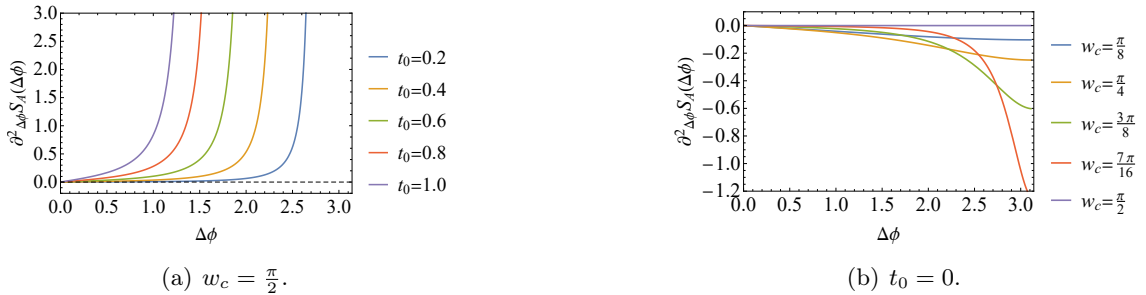


Figure 12. The second-order derivative of the entanglement entropy. 12(a) we take $w_c = \frac{\pi}{2}$, with $r_{\text{eff}} = \ell_{\text{dS}} \cosh t_0 \sin \frac{\Delta\phi}{2}$. In this case, we need to always ensure that $\cosh t_0 \sin \frac{\Delta\phi}{2} < 1$. 12(b) we take $t_0 = 0$, with $r_{\text{eff}} = \ell_{\text{dS}} \sin w_c \sin \frac{\Delta\phi}{2} < \ell_{\text{dS}}$.

For the two cases described above, the boundary positions are illustrated in figure. 13. The orange region corresponds to $\sin w_c \cosh t_0 > 1$, where the dual field theory is nonlocal. The blue region corresponds to $\sin w_c \cosh t_0 < 1$, where the dual field theory satisfies the strong subadditivity inequality. However, it can be proven that in this case, the entanglement entropy does not satisfy the boosted strong subadditivity inequality. In the dS₂ background, the infinitesimal form of the boosted strong subadditivity inequality is given by [62]

$$\text{BSSA}(\Delta\phi) = \partial_{\Delta\phi}^2 S_A(\Delta\phi) + \frac{1}{\sin \Delta\phi} \partial_{\Delta\phi} S_A(\Delta\phi) \leq 0. \quad (5.19)$$

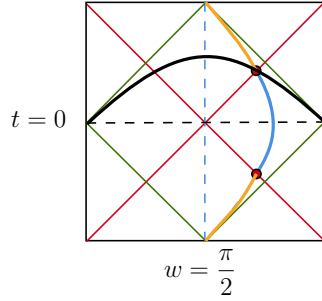


Figure 13. The Penrose diagram of dS/dS correspondence. The black and blue dashed lines represent the codimension-one hypersurfaces at $t = 0$ and $w = \frac{\pi}{2}$, respectively. The black curve represents the spacelike hypersurface at $t = t_0$, and the orange and blue curves represent the dS slices at $w = w_c$, where the dual field theory is located. The intersection of these two hypersurfaces corresponds to the critical case that saturates the strong subadditivity inequality, where $\sin w_c \cosh t_0 = 1$.

By substituting eq. (5.17) into the left-hand side of the boosted strong subadditivity inequality (5.19), we obtain

$$\text{BSSA}(\Delta\phi) = \frac{c_{\text{dS}}}{48} \frac{\sin^2 \Delta\phi}{\sin^6 \frac{\Delta\phi}{2} \sin^2 w_c \left(\frac{1}{\sin^2 \frac{\Delta\phi}{2} \sin^2 w_c} - 1 \right)^{\frac{3}{2}}} > 0, \quad (5.20)$$

which indicates that, in this case, the dual field theory remains nonlocal. In particular, at the ultraviolet boundary where $w_c = \frac{\pi}{2}$, there is a significant violation of the boosted strong subadditivity inequality, as indicated by the purple line in figure 14.

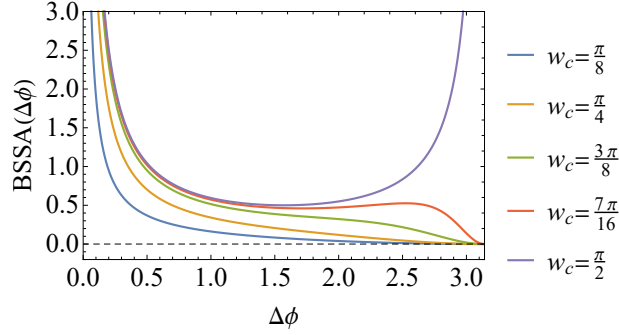


Figure 14. The boosted strong subadditivity inequality violate in the dS/dS holography.

5.3 The half-dS holography

By introducing a timelike boundary $\Theta = \Theta_0$ in dS global spacetime, the half-dS holographic model was obtained in ref. [65]. The dual field theory resides on the timelike boundary, and the bulk spacetime is confined to the region where $0 < \Theta < \Theta_0$. The induced metric on the boundary is given by

$$ds^2 = \ell_{\text{dS}}^2 (-dt^2 + \cosh^2 t \sin^2 \Theta_0 d\Phi^2). \quad (5.21)$$

By rescaling the coordinate t in a manner analogous to that discussed in Section 5.1, we obtain the conformal cylindrical metric

$$ds^2 = \ell_{\text{dS}}^2 \frac{\sin^2 \Theta_0}{\cosh^2(\tilde{t} \sin \Theta_0)} (d\tilde{t}^2 + d\Phi^2), \quad (5.22)$$

where the coordinate transformation between \tilde{t} and t is

$$\tilde{t} = \frac{1}{\sin \Theta_0} \ln \frac{\cot \frac{t}{2} + 1}{\cot \frac{t}{2} - 1}. \quad (5.23)$$

Mapping from the cylinder to the plane as in eq. (5.4), the metric transforms into a conformally flat form

$$ds^2 = \frac{\ell_{\text{dS}}^2 \sin^2 \Theta_0}{\cosh^2(\ln(\sqrt{T^2 + X^2}) \sin \Theta_0)} \frac{dT^2 + dX^2}{T^2 + X^2}. \quad (5.24)$$

Next, we calculate the entanglement entropy for the subregion interval $(-\Phi_a, \Phi_a)$ at $t = t_0$. After the mapping, the coordinates of the subregion endpoints are

$$(T_1, X_1) = \left(e^{\tilde{t}_0} \cos \Phi_a, -e^{\tilde{t}_0} \sin \Phi_a \right), \quad (T_2, X_2) = \left(e^{\tilde{t}_0} \cos \Phi_a, e^{\tilde{t}_0} \sin \Phi_a \right). \quad (5.25)$$

Using the CHM mapping,

$$T \rightarrow \frac{e^{\tilde{t}_0} \sin \Phi_a \sin \theta \sin \phi}{1 + \sin \theta \cos \phi} + e^{\tilde{t}_0} \cos \Phi_a, \quad X \rightarrow \frac{e^{\tilde{t}_0} \sin \Phi_a \cos \theta}{1 + \sin \theta \cos \phi}, \quad (5.26)$$

we obtain the conformal spherical metric

$$ds^2 = \frac{2\Omega^2 \ell_{\text{dS}}^2 \sin^2 \Theta_0 \sin^2 \Phi_a (d\theta^2 + \sin^2 \theta d\phi^2)}{(1 + \sin \theta \cos \phi)(2 + \sin(\theta + \phi - 2\Phi_a) + \sin(\theta - \phi + 2\Phi_a))}, \quad (5.27)$$

where

$$\Omega^{-1} = \cosh \left(\frac{1}{2} \ln \left(\frac{e^{2\tilde{t}_0} (2 + \sin(\theta + \phi - 2\Phi_a) + \sin(\theta - \phi + 2\Phi_a))}{2 + 2 \sin \theta \cos \phi} \right) \sin \Theta_0 \right). \quad (5.28)$$

At the endpoints ($\theta = 0, \pi$), the conformal factor becomes $\cosh^{-1} \tilde{t}_0$. Thus, the effective radius of the sphere in the Lorentzian signature is

$$r_{\text{eff}} = \ell_{\text{dS}} \cosh t_0 \sin \Theta_0 \sin \Phi_a. \quad (5.29)$$

Therefore, the entanglement entropy is

$$S = \frac{c_{\text{dS}}}{3} \arctan \left(\frac{1}{\sqrt{\frac{c_{\text{dS}} \lambda_{\text{dS}}}{12r_{\text{eff}}^2} - 1}} \right) = \frac{c_{\text{dS}}}{3} \arctan \left(\frac{1}{\sqrt{\frac{1}{(\cosh t_0 \sin \Theta_0 \sin \Phi_a)^2} - 1}} \right). \quad (5.30)$$

In the case of $t_0 = 0$ and $\Theta_0 = \frac{\pi}{2}$, the radius in the spherical partition function is $r_{\text{eff}} = \ell_{\text{dS}} \sin \frac{\Delta\Phi}{2}$, where $\Delta\Phi = |-\Phi_a - \Phi_a| = 2\Phi_a$. The entanglement entropy is

$$S = \frac{c_{\text{dS}}}{3} \arctan \left(\frac{1}{\sqrt{\frac{c_{\text{dS}} \lambda_{\text{dS}}}{12r_{\text{eff}}^2} - 1}} \right) = \frac{c_{\text{dS}}}{3} \arctan \left(\frac{1}{\sqrt{\frac{1}{\sin^2 \frac{\Delta\Phi}{2}} - 1}} \right) = \frac{c_{\text{dS}}}{6} \Delta\Phi. \quad (5.31)$$

By replacing the field theory parameter c_{dS} with the gravitational parameter $\frac{3\ell_{\text{dS}}}{2G}$, we find that the above result matches the holographic calculation presented in ref. [65], confirming the validity of the half-dS holography. Additionally, the requirement that the effective radius of the sphere be smaller than the cosmological horizon aligns precisely with the condition given in eq. (3.6) of ref. [65] to ensure the existence of spacelike geodesics:

$$r_{\text{eff}} = \ell_{\text{dS}} \cosh t_0 \sin \Theta_0 \sin \frac{\Delta\Phi}{2} \leq \ell_{\text{dS}}. \quad (5.32)$$

In ref. [65], the dual field theory in the half-dS holography was proposed to exhibit non-locality. It was concluded that when $\cosh t_0 \leq \frac{1}{\sin \Theta_0}$, the entanglement entropy satisfies the strong subadditivity inequality, whereas when $\cosh t_0 > \frac{1}{\sin \Theta_0}$, the strong subadditivity inequality is violated. As shown in figure 15, the orange line segment represents the region where the strong subadditivity inequality is violated, while the blue line segment represents the region where the strong subadditivity inequality is satisfied. Next, we demonstrate that even in the blue region where the strong subadditivity inequality is satisfied, the boosted strong subadditivity inequality is still violated.

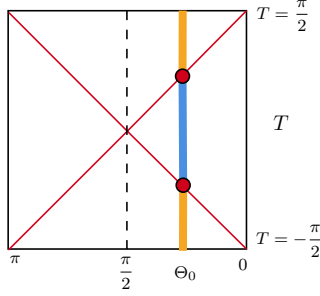


Figure 15. The half-dS holography. The dual field theory resides on a timelike boundary at $\Theta = \Theta_0$, while the bulk spacetime covers the region $0 < \Theta < \Theta_0$. Here we set $\cos T = \frac{1}{\cosh t}$. The blue intervals indicate $\cosh t \leq \frac{1}{\sin \Theta_0}$, i.e., $\Theta_0 - \frac{\pi}{2} \leq T \leq \frac{\pi}{2} - \Theta_0$.

By observing eqs. (5.15) and (5.30), we find that the results from calculating the spatial interval entanglement entropy in the dS/dS holography and half-dS holography are similar. However, due to the difference in boundary-induced metrics, the boosted strong subadditivity inequality receives corresponding corrections. In the half-dS holography, the infinitesimal form of the boosted strong subadditivity inequality is

$$\text{BSSA}(\Delta\tilde{\Phi}) = \sin^2 \Theta_0 \left(\partial_{\Delta\tilde{\Phi}}^2 S(\Delta\tilde{\Phi}) + \frac{1}{\sin \Delta\tilde{\Phi}} \partial_{\Delta\tilde{\Phi}} S(\Delta\tilde{\Phi}) \right) \leq 0, \quad (5.33)$$

where $\Delta\tilde{\Phi} = \sin \Theta_0 \Delta\Phi$. Substituting the result for the entanglement entropy into the above expression, we can get

$$\text{BSSA}(\Delta\phi) = \frac{c_{\text{dS}}}{48} \frac{\sin^2(\Delta\phi \sin \Theta_0)}{\sin^6(\frac{1}{2}\Delta\phi \sin \Theta_0) \left(\frac{1}{\sin^2 \Theta_0 \sin^2(\frac{1}{2}\Delta\phi \sin \Theta_0)} - 1 \right)^{\frac{3}{2}}} > 0. \quad (5.34)$$

The result is illustrated in figure 16, which indicates that, in the half-dS holography, the boundary field theory still does not satisfy the boosted strong subadditivity inequality.

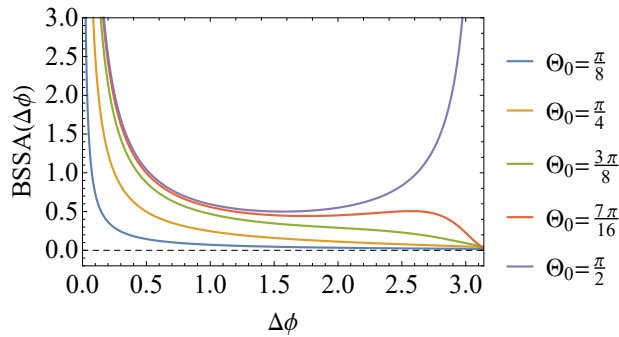


Figure 16. The boosted strong subadditivity inequality violates in the half-dS holography.

We have calculated the entanglement entropy of subsystem A using the generalized spherical partition function method within the dS/dS correspondence and half-dS holography frameworks. Furthermore, we have reaffirmed the conclusions from Section 3.2 by applying the

boosted strong subadditivity inequality and the strong subadditivity inequality: in dS_3 space-time, when the effective radius of the sphere is smaller than the cosmological horizon, the dual field theory exhibits non-locality.

6 Conclusion and Discussion

This paper investigated the effects of the $T\bar{T}$ deformation on various holographic dualities, including AdS/CFT, dS/CFT, and dS/dS, by analyzing the entanglement entropy of the boundary field theory. When the boundary is spherical, and the subsystem is a semicircular arc, the entanglement entropy can be derived from the classical partition function on the n -replica manifold, with the partition function governed by the trace flow equation.

To study the entanglement entropy in the dS case, we first derived the trace flow equation for the dS/CFT by applying a double Wick rotation to the AdS case. Then, we considered a simple scenario where the subsystem is a semicircular arc on the sphere, which corresponds to global coordinates in the dS/CFT, as well as the $t = 0$ moment in both AdS/dS and dS/dS. Our findings are as follows:

- In dS/CFT, the entanglement entropy is complex, indicating that the dual field theory is non-unitary.
- In dS/dS, the entanglement entropy is real but violates the strong subadditivity inequality, suggesting that the dual field theory is unitary but non-local.

We then examined a more complicated scenario where the boundary-induced metric is time-dependent, covering AdS/dS, dS/dS, and half-dS holography. In these cases, since the expressions for the strong subadditivity inequality and the boosted strong subadditivity inequality depend on the specific form of the metric, and the boundary-induced metric is time-dependent, the locality of the boundary field theory may vary across different time periods, as discussed in ref. [65]. To address this, we further generalized the replica method on the sphere to accommodate more general manifolds and subsystems. We first verified this method in the global coordinates of AdS/CFT, dS/CFT, and the planar BTZ case, where the results are consistent with existing perturbative calculations [16, 79]. We then applies it to the cases where the boundary-induced metrics are time-dependent. Our results show that while the subsystem's entanglement entropy may satisfy the strong subadditivity inequality at certain time periods in dS/dS and half-dS holographies, the boosted strong subadditivity inequality is consistently violated, indicating that the dual field theories remain non-local throughout.

Acknowledgments

We would like to thank Shan-Ming Ruan for reading our draft and providing comments. We also thank Yang He, and Shan-Ping Wu for their helpful discussion. This work was supported by the National Natural Science Foundation of China (Grants No. 12475056, No.

12235016, No. 12075101, No. 12475053, and No. 12247101), the 111 Project under (Grant No. B20063), the Major Science and Technology Projects of Gansu Province, and Lanzhou City’s scientific research funding subsidy to Lanzhou University. S.H. would appreciate the financial support from the Fundamental Research Funds for the Central Universities and Max Planck Partner Group and the Natural Science Foundation of China (NSFC) Grants No. 12075101 and No. 12235016. L.Z. is supported by the Science and Technology Development Plan Project of Jilin Province, China (No. 20240101326JC).

A The gravity calculation

A.1 The dS/Poincaré case

In the dS Poincaré spacetime,

$$ds^2 = \frac{\ell_{\text{dS}}^2}{\eta^2} (-d\eta^2 + dX^2 + dT^2), \quad (\text{A.1})$$

the geodesic distance D_{12} between two points “1” $(\eta, X, T) = (\eta_c, -X_a, 0)$ and “2” $(\eta_c, -X_a, 0)$ can be desolved by

$$\cos \frac{D_{12}}{\ell_{\text{dS}}} = -V_1 V_2 + U_1 U_2 + Y_1 Y_2 + W_1 W_2. \quad (\text{A.2})$$

The uppercase coordinates “ U, Y, W, V ” denote the coordinates of the embedded spacetime

$$ds^2 = -dV^2 + dW^2 + dU^2 + dY^2. \quad (\text{A.3})$$

The dS spacetime is a codimensional one hypersurface in the embedded spacetime

$$-V^2 + W^2 + U^2 + Y^2 = \ell_{\text{dS}}^2, \quad (\text{A.4})$$

and they adhere to the following transformation relations with respect to the coordinates of the dS spacetime itself

$$\begin{aligned} U &= \frac{\ell_{\text{dS}}}{\eta} X, & V &= \ell_{\text{dS}} \sinh\left(\log\left(\frac{\ell_{\text{dS}}}{\eta}\right)\right) + \frac{1}{\eta} \frac{X^2 + T^2}{2}, \\ Y &= \frac{\ell_{\text{dS}}}{\eta} T, & W &= \ell_{\text{dS}} \cosh\left(\log\left(\frac{\ell_{\text{dS}}}{\eta}\right)\right) - \frac{1}{\eta} \frac{X^2 + T^2}{2}. \end{aligned} \quad (\text{A.5})$$

Finally we can get the geodesic distance is

$$D_{12} = \ell_{\text{dS}} \arccos \left(\ell_{\text{dS}}^2 \left(1 - \frac{2X_a^2}{\eta_c^2} \right) \right) \simeq -2i\ell_{\text{dS}} \log \frac{2X_a}{\eta_c} + i\ell_{\text{dS}} \frac{\eta_c^2}{2X_a^2} + \pi\ell_{\text{dS}}. \quad (\text{A.6})$$

So the entanglement entropy of the subregion is

$$S = \frac{D_{12}}{4G} \simeq -\frac{ic_{\text{dS}}}{3} \log \frac{2X_a}{\eta_c} + \frac{ic_{\text{dS}}\eta_c^2}{12X_a^2} + \frac{\pi c_{\text{dS}}}{6}. \quad (\text{A.7})$$

This is consistent with eq. (4.17).

A.2 The global dS case

For the dS global coordinates, the coordinate transformation in embedding spacetime is

$$\begin{aligned} U &= \ell_{\text{dS}} \cosh t \sin \Theta \cos \Phi, & V &= \ell_{\text{dS}} \sinh t, \\ Y &= \ell_{\text{dS}} \cosh t \sin \Theta \sin \Phi, & W &= \ell_{\text{dS}} \cosh t \cos \Theta. \end{aligned} \quad (\text{A.8})$$

So the geodesic distance of two points $(t, \Theta, \Phi)=(t_1, \Theta_1, \Phi_1), (t_2, \Theta_2, \Phi_2)$ in the dS global coordinates is

$$\cos \frac{D_{12}}{\ell_{\text{dS}}} = (\cos \Theta_1 \cos \Theta_2 + \sin \Theta_1 \sin \Theta_2 \cos(\Phi_1 - \Phi_2)) \cosh t_1 \cosh t_2 - \sinh t_1 \sinh t_2. \quad (\text{A.9})$$

Now we can select the endpoints of the subsystem as $(t, \Theta, \Phi)=(t_c, \frac{\pi}{2}, -\Phi_a), (t_c, \frac{\pi}{2}, \Phi_a)$, so we have

$$D_{12} = \ell_{\text{dS}} \cos^{-1} (\cos(2\Phi_a) \cosh^2 t_c - \sinh^2 t_c) = \ell_{\text{dS}} \cos^{-1} (1 - 2 \cosh^2 t_c \sin^2 \Phi_a). \quad (\text{A.10})$$

Considering that the finite cutoff t_c tends to infinity, we expand the above results to the second-order

$$D_{12} \simeq -2i\ell_{\text{dS}} \log(2 \cosh t_c \sin \Phi_a) + \frac{i\ell_{\text{dS}}}{2 \cosh^2 t_c \sin^2 \Phi_a} + \pi\ell_{\text{dS}}. \quad (\text{A.11})$$

Finally, we have the entanglement entropy

$$S = \frac{D_{12}}{4G} \simeq -\frac{ic_{\text{dS}}}{3} \log(2 \cosh t_c \sin \Phi_a) + \frac{ic_{\text{dS}}}{12 \cosh^2 t_c \sin^2 \Phi_a} + \frac{\pi c_{\text{dS}}}{6}. \quad (\text{A.12})$$

We can get the same result as eq. (4.34).

References

- [1] F.A. Smirnov and A.B. Zamolodchikov, *On space of integrable quantum field theories*, *Nucl. Phys. B* **915** (2017) 363 [[1608.05499](#)].
- [2] A. Cavaglià, S. Negro, I.M. Szécsényi and R. Tateo, *$T\bar{T}$ -deformed 2D Quantum Field Theories*, *JHEP* **10** (2016) 112 [[1608.05534](#)].
- [3] A.B. Zamolodchikov, *Expectation value of composite field T anti- T in two-dimensional quantum field theory*, [hep-th/0401146](#).
- [4] Y. Jiang, *Expectation value of $T\bar{T}$ operator in curved spacetimes*, *JHEP* **02** (2020) 094 [[1903.07561](#)].
- [5] J.M. Maldacena, *The Large N limit of superconformal field theories and supergravity*, *Adv. Theor. Math. Phys.* **2** (1998) 231 [[hep-th/9711200](#)].
- [6] S.S. Gubser, I.R. Klebanov and A.M. Polyakov, *Gauge theory correlators from noncritical string theory*, *Phys. Lett. B* **428** (1998) 105 [[hep-th/9802109](#)].
- [7] E. Witten, *Anti-de Sitter space and holography*, *Adv. Theor. Math. Phys.* **2** (1998) 253 [[hep-th/9802150](#)].

- [8] L. McGough, M. Mezei and H. Verlinde, *Moving the CFT into the bulk with $T\bar{T}$* , *JHEP* **04** (2018) 010 [[1611.03470](#)].
- [9] P. Kraus, J. Liu and D. Marolf, *Cutoff AdS_3 versus the $T\bar{T}$ deformation*, *JHEP* **07** (2018) 027 [[1801.02714](#)].
- [10] S. He, Y. Li, Y.-Z. Li and Y. Zhang, *Holographic torus correlators of stress tensor in AdS_3/CFT_2* , *JHEP* **06** (2023) 116 [[2303.13280](#)].
- [11] S. He, Y.-Z. Li and Y. Zhang, *Holographic torus correlators in AdS_3 gravity coupled to scalar field*, *JHEP* **05** (2024) 254 [[2311.09636](#)].
- [12] S. He, Y. Li, Y.-Z. Li and Y. Zhang, *Note on holographic torus stress tensor correlators in AdS_3 gravity*, [2405.01255](#).
- [13] S. He, Y.-Z. Li and Y. Xie, *Holographic stress tensor correlators on higher genus Riemann surfaces*, [2406.04042](#).
- [14] V.E. Hubeny, M. Rangamani and T. Takayanagi, *A Covariant holographic entanglement entropy proposal*, *JHEP* **07** (2007) 062 [[0705.0016](#)].
- [15] S. Ryu and T. Takayanagi, *Holographic derivation of entanglement entropy from AdS/CFT* , *Phys. Rev. Lett.* **96** (2006) 181602 [[hep-th/0603001](#)].
- [16] B. Chen, L. Chen and P.-X. Hao, *Entanglement entropy in $T\bar{T}$ -deformed CFT*, *Phys. Rev. D* **98** (2018) 086025 [[1807.08293](#)].
- [17] H.-S. Jeong, K.-Y. Kim and M. Nishida, *Entanglement and Rényi entropy of multiple intervals in $T\bar{T}$ -deformed CFT and holography*, *Phys. Rev. D* **100** (2019) 106015 [[1906.03894](#)].
- [18] Y. Jiang, *A pedagogical review on solvable irrelevant deformations of 2D quantum field theory*, *Commun. Theor. Phys.* **73** (2021) 057201 [[1904.13376](#)].
- [19] K. Allameh, A.F. Astaneh and A. Hassanzadeh, *Aspects of holographic entanglement entropy for $T\bar{T}$ -deformed CFTs*, *Phys. Lett. B* **826** (2022) 136914 [[2111.11338](#)].
- [20] M.R. Setare and S.N. Sajadi, *Holographic entanglement entropy in $T\bar{T}$ -deformed CFTs*, *Gen. Rel. Grav.* **54** (2022) 85 [[2203.16445](#)].
- [21] M. He and Y. Sun, *Holographic entanglement entropy in $T\bar{T}$ -deformed AdS_3* , *Nucl. Phys. B* **990** (2023) 116190 [[2301.04435](#)].
- [22] L. Apolo, P.-X. Hao, W.-X. Lai and W. Song, *Extremal surfaces in glue-on $AdS/T\bar{T}$ holography*, *JHEP* **01** (2024) 054 [[2311.04883](#)].
- [23] X. Jiang, P. Wang, H. Wu and H. Yang, *Timelike entanglement entropy and $T\bar{T}$ deformation*, *Phys. Rev. D* **108** (2023) 046004 [[2302.13872](#)].
- [24] Z. Li, Z.-Q. Xiao and R.-Q. Yang, *On holographic time-like entanglement entropy*, *JHEP* **04** (2023) 004 [[2211.14883](#)].
- [25] K. Doi, J. Harper, A. Mollabashi, T. Takayanagi and Y. Taki, *Timelike entanglement entropy*, *JHEP* **05** (2023) 052 [[2302.11695](#)].
- [26] S. Dutta and T. Faulkner, *A canonical purification for the entanglement wedge cross-section*, *JHEP* **03** (2021) 178 [[1905.00577](#)].

- [27] Y. Nakata, T. Takayanagi, Y. Taki, K. Tamaoka and Z. Wei, *New holographic generalization of entanglement entropy*, *Phys. Rev. D* **103** (2021) 026005 [[2005.13801](#)].
- [28] D. Basu and V. Raj, *Reflected entropy and timelike entanglement in $T\bar{T}$ deformed CFT_2 s*, [2402.07253](#).
- [29] S. He, J. Yang, Y.-X. Zhang and Z.-X. Zhao, *Pseudo entropy of primary operators in $T\bar{T}/J\bar{T}$ -deformed CFTs*, *JHEP* **09** (2023) 025 [[2305.10984](#)].
- [30] S. He and H. Shu, *Correlation functions, entanglement and chaos in the $T\bar{T}/J\bar{T}$ -deformed CFTs*, *JHEP* **02** (2020) 088 [[1907.12603](#)].
- [31] M. Asrat and J. Kudler-Flam, *$T\bar{T}$, the entanglement wedge cross section, and the breakdown of the split property*, *Phys. Rev. D* **102** (2020) 045009 [[2005.08972](#)].
- [32] S. Khoeini-Moghaddam, F. Omid and C. Paul, *Aspects of Holographic Violating Geometries at Finite Cutoff*, *JHEP* **02** (2021) 121 [[2011.00305](#)].
- [33] Y. Li and Y. Zhou, *Cutoff AdS_3 versus $T\bar{T}$ CFT_2 in the large central charge sector: correlators of energy-momentum tensor*, *JHEP* **12** (2020) 168 [[2005.01693](#)].
- [34] H.-S. Jeong, W.-B. Pan, Y.-W. Sun and Y.-T. Wang, *Holographic study of $T\bar{T}$ like deformed HV QFTs: holographic entanglement entropy*, *JHEP* **02** (2023) 018 [[2211.00518](#)].
- [35] M. He, J. Hou and Y. Jiang, *$T\bar{T}$ -deformed entanglement entropy for IQFT*, *JHEP* **03** (2024) 056 [[2306.07784](#)].
- [36] J. Tian, *On-shell action of $T\bar{T}$ -deformed Holographic CFTs*, [2306.01258](#).
- [37] L. Apolo, P.-X. Hao, W.-X. Lai and W. Song, *Glue-on AdS holography for $T\bar{T}$ -deformed CFTs*, *JHEP* **06** (2023) 117 [[2303.04836](#)].
- [38] D. Basu, Lavish and B. Paul, *Entanglement negativity in $T\bar{T}$ -deformed CFT_2 s*, *Phys. Rev. D* **107** (2023) 126026 [[2302.11435](#)].
- [39] D. Basu, S. Biswas, A. Dey, B. Paul and G. Sengupta, *Odd entanglement entropy in $T\bar{T}$ deformed CFT_2 s and holography*, *Phys. Rev. D* **108** (2023) 126013 [[2307.04832](#)].
- [40] M. He, *One-loop partition functions in $T\bar{T}$ -deformed AdS_3* , *JHEP* **05** (2024) 067 [[2401.09879](#)].
- [41] E. Tsolakidis, *Massive gravity generalization of $T\bar{T}$ deformations*, [2405.07967](#).
- [42] H. Babaei-Aghbolagh, S. He, T. Morone, H. Ouyang and R. Tateo, *Geometric Formulation of Generalized Root- $T\bar{T}$ Deformations*, *Phys. Rev. Lett.* **133** (2024) 111602 [[2405.03465](#)].
- [43] E. Witten, *Quantum gravity in de Sitter space*, in *Strings 2001: International Conference*, 6, 2001 [[hep-th/0106109](#)].
- [44] J.M. Maldacena, *Non-Gaussian features of primordial fluctuations in single field inflationary models*, *JHEP* **05** (2003) 013 [[astro-ph/0210603](#)].
- [45] M. Miyaji and T. Takayanagi, *Surface/State Correspondence as a Generalized Holography*, *PTEP* **2015** (2015) 073B03 [[1503.03542](#)].
- [46] X. Jiang, P. Wang, H. Wu and H. Yang, *Timelike entanglement entropy in dS_3/CFT_2* , *JHEP* **08** (2023) 216 [[2304.10376](#)].
- [47] J.-C. Chang, S. He, Y.-X. Liu and L. Zhao, *Island formula in Planck brane*, *JHEP* **11** (2023) 006 [[2308.03645](#)].

- [48] H.-Y. Chen, Y. Hikida, Y. Taki and T. Uetoko, *Complex saddles of three-dimensional de Sitter gravity via holography*, *Phys. Rev. D* **107** (2023) L101902 [2302.09219].
- [49] K. Doi, N. Ogawa, K. Shinmyo, Y.-k. Suzuki and T. Takayanagi, *Probing de Sitter Space Using CFT States*, [2405.14237](#).
- [50] A. Strominger, *The dS / CFT correspondence*, *JHEP* **10** (2001) 034 [[hep-th/0106113](#)].
- [51] A. Strominger, *Inflation and the dS / CFT correspondence*, *JHEP* **11** (2001) 049 [[hep-th/0110087](#)].
- [52] K. Doi, J. Harper, A. Mollabashi, T. Takayanagi and Y. Taki, *Pseudoentropy in dS /CFT and Timelike Entanglement Entropy*, *Phys. Rev. Lett.* **130** (2023) 031601 [2210.09457].
- [53] D. Anninos, T. Hartman and A. Strominger, *Higher Spin Realization of the dS /CFT Correspondence*, *Class. Quant. Grav.* **34** (2017) 015009 [1108.5735].
- [54] G.S. Ng and A. Strominger, *State/Operator Correspondence in Higher-Spin dS /CFT*, *Class. Quant. Grav.* **30** (2013) 104002 [1204.1057].
- [55] Y. Hikida, T. Nishioka, T. Takayanagi and Y. Taki, *CFT duals of three-dimensional de Sitter gravity*, *JHEP* **05** (2022) 129 [2203.02852].
- [56] Y. Hikida, T. Nishioka, T. Takayanagi and Y. Taki, *Holography in de Sitter Space via Chern-Simons Gauge Theory*, *Phys. Rev. Lett.* **129** (2022) 041601 [2110.03197].
- [57] H.-Y. Chen and Y. Hikida, *Three-Dimensional de Sitter Holography and Bulk Correlators at Late Time*, *Phys. Rev. Lett.* **129** (2022) 061601 [2204.04871].
- [58] M. Alishahiha, A. Karch, E. Silverstein and D. Tong, *The dS/dS correspondence*, *AIP Conf. Proc.* **743** (2004) 393 [[hep-th/0407125](#)].
- [59] M. Alishahiha, A. Karch and E. Silverstein, *Hologravity*, *JHEP* **06** (2005) 028 [[hep-th/0504056](#)].
- [60] X. Dong, E. Silverstein and G. Torroba, *De Sitter Holography and Entanglement Entropy*, *JHEP* **07** (2018) 050 [1804.08623].
- [61] H. Geng, S. Grienering and A. Karch, *Entropy, Entanglement and Swampland Bounds in DS/dS* , *JHEP* **06** (2019) 105 [1904.02170].
- [62] H. Geng, *Some Information Theoretic Aspects of De-Sitter Holography*, *JHEP* **02** (2020) 005 [1911.02644].
- [63] H. Geng, *Non-local entanglement and fast scrambling in de-Sitter holography*, *Annals Phys.* **426** (2021) 168402 [2005.00021].
- [64] H. Geng, Y. Nomura and H.-Y. Sun, *Information paradox and its resolution in de Sitter holography*, *Phys. Rev. D* **103** (2021) 126004 [2103.07477].
- [65] T. Kawamoto, S.-M. Ruan, Y.-k. Suzuki and T. Takayanagi, *A half de Sitter holography*, *JHEP* **10** (2023) 137 [2306.07575].
- [66] V. Gorbenko, E. Silverstein and G. Torroba, *dS/dS and $T\bar{T}$* , *JHEP* **03** (2019) 085 [1811.07965].
- [67] V. Shyam, *$T\bar{T} + \Lambda_2$ deformed CFT on the stretched dS_3 horizon*, *JHEP* **04** (2022) 052 [2106.10227].

- [68] E. Coleman, E.A. Mazenc, V. Shyam, E. Silverstein, R.M. Soni, G. Torroba et al., *De Sitter microstates from $T\bar{T} + \Lambda_2$ and the Hawking-Page transition*, *JHEP* **07** (2022) 140 [[2110.14670](#)].
- [69] G. Torroba, *$T\bar{T} + \Lambda_2$ from a 2d gravity path integral*, *JHEP* **01** (2023) 163 [[2212.04512](#)].
- [70] G. Batra, G.B. De Luca, E. Silverstein, G. Torroba and S. Yang, *Bulk-local dS_3 holography: the Matter with $T\bar{T} + \Lambda_2$* , [2403.01040](#).
- [71] P. Calabrese and J. Cardy, *Entanglement entropy and conformal field theory*, *J. Phys. A* **42** (2009) 504005 [[0905.4013](#)].
- [72] W. Donnelly and V. Shyam, *Entanglement entropy and $T\bar{T}$ deformation*, *Phys. Rev. Lett.* **121** (2018) 131602 [[1806.07444](#)].
- [73] P. Caputa, S. Datta and V. Shyam, *Sphere partition functions | \mathcal{E} cut-off AdS*, *JHEP* **05** (2019) 112 [[1902.10893](#)].
- [74] F. Deng, Z. Wang and Y. Zhou, *End of the World Brane meets $T\bar{T}$* , [2310.15031](#).
- [75] K.G. Wilson and J.B. Kogut, *The Renormalization group and the epsilon expansion*, *Phys. Rept.* **12** (1974) 75.
- [76] J. Polchinski, *Renormalization and Effective Lagrangians*, *Nucl. Phys. B* **231** (1984) 269.
- [77] A. Lewkowycz and J. Maldacena, *Generalized gravitational entropy*, *JHEP* **08** (2013) 090 [[1304.4926](#)].
- [78] A. Lewkowycz, J. Liu, E. Silverstein and G. Torroba, *$T\bar{T}$ and EE, with implications for (A)dS subregion encodings*, *JHEP* **04** (2020) 152 [[1909.13808](#)].
- [79] D. Chen, X. Jiang and H. Yang, *Holographic $T\bar{T}$ deformed entanglement entropy in dS_3/CFT_2* , [2307.04673](#).
- [80] H. Casini, M. Huerta and R.C. Myers, *Towards a derivation of holographic entanglement entropy*, *JHEP* **05** (2011) 036 [[1102.0440](#)].
- [81] J.D. Brown and M. Henneaux, *Central charges in the canonical realization of asymptotic symmetries: An example from three dimensional gravity*, *Commun. Math. Phys.* **104** (1986) 207.
- [82] V. Shyam, *Background independent holographic dual to $T\bar{T}$ deformed CFT with large central charge in 2 dimensions*, *JHEP* **10** (2017) 108 [[1707.08118](#)].
- [83] T. Hartman, J. Kruthoff, E. Shaghoulian and A. Tajdini, *Holography at finite cutoff with a T^2 deformation*, *JHEP* **03** (2019) 004 [[1807.11401](#)].
- [84] V. Balasubramanian and P. Kraus, *A Stress tensor for Anti-de Sitter gravity*, *Commun. Math. Phys.* **208** (1999) 413 [[hep-th/9902121](#)].
- [85] C. Fefferman and C.R. Graham, *Conformal invariants, in Élie Cartan et les mathématiques d'aujourd'hui - Lyon, 25-29 juin 1984* **Astérisque** (1985) 95.
- [86] R.L. Arnowitt, S. Deser and C.W. Misner, *The Dynamics of general relativity*, *Gen. Rel. Grav.* **40** (2008) 1997 [[gr-qc/0405109](#)].
- [87] E. Witten, *A Note On The Canonical Formalism for Gravity*, [2212.08270](#).

- [88] B.S. DeWitt, *Quantum Theory of Gravity. 1. The Canonical Theory*, *Phys. Rev.* **160** (1967) 1113.
- [89] X. Dong, G.N. Remmen, D. Wang, W.W. Weng and C.-H. Wu, *Holographic entanglement from the UV to the IR*, [2308.07952](#).
- [90] M. Headrick, *Entanglement Renyi entropies in holographic theories*, *Phys. Rev. D* **82** (2010) 126010 [[1006.0047](#)].
- [91] L.-Y. Hung, R.C. Myers, M. Smolkin and A. Yale, *Holographic Calculations of Renyi Entropy*, *JHEP* **12** (2011) 047 [[1110.1084](#)].
- [92] S. Griener, *Entanglement entropy and $T\bar{T}$ deformations beyond antipodal points from holography*, *JHEP* **11** (2019) 171 [[1908.10372](#)].
- [93] H. Casini and M. Huerta, *On the RG running of the entanglement entropy of a circle*, *Phys. Rev. D* **85** (2012) 125016 [[1202.5650](#)].
- [94] H. Casini and M. Huerta, *A Finite entanglement entropy and the c-theorem*, *Phys. Lett. B* **600** (2004) 142 [[hep-th/0405111](#)].
- [95] E. Barnes, K.A. Intriligator, B. Wecht and J. Wright, *Evidence for the strongest version of the 4d a-theorem, via a-maximization along RG flows*, *Nucl. Phys. B* **702** (2004) 131 [[hep-th/0408156](#)].
- [96] S. Gukov, *Counting RG flows*, *JHEP* **01** (2016) 020 [[1503.01474](#)].
- [97] A.B. Zamolodchikov, *Irreversibility of the Flux of the Renormalization Group in a 2D Field Theory*, *JETP Lett.* **43** (1986) 730.
- [98] J. de Boer, E.P. Verlinde and H.L. Verlinde, *On the holographic renormalization group*, *JHEP* **08** (2000) 003 [[hep-th/9912012](#)].
- [99] E.P. Verlinde and H.L. Verlinde, *RG flow, gravity and the cosmological constant*, *JHEP* **05** (2000) 034 [[hep-th/9912018](#)].
- [100] I. Heemskerk and J. Polchinski, *Holographic and Wilsonian Renormalization Groups*, *JHEP* **06** (2011) 031 [[1010.1264](#)].
- [101] T. Nishioka, *Entanglement entropy: holography and renormalization group*, *Rev. Mod. Phys.* **90** (2018) 035007 [[1801.10352](#)].
- [102] S. Griener, K. Ikeda and D.E. Kharzeev, *Temporal entanglement entropy as a probe of renormalization group flow*, *JHEP* **05** (2024) 030 [[2312.08534](#)].
- [103] H. Kamei, *Notes on the Exact RG equation and the Wheeler-DeWitt equation*, [2402.16100](#).
- [104] Y. Nakayama, *Scale invariance vs conformal invariance*, *Phys. Rept.* **569** (2015) 1 [[1302.0884](#)].
- [105] M. Banados, C. Teitelboim and J. Zanelli, *The Black hole in three-dimensional space-time*, *Phys. Rev. Lett.* **69** (1992) 1849 [[hep-th/9204099](#)].